

AD-760 178

TECHNOLOGY DEVELOPMENT FOR TRANSITION  
METAL-RARE EARTH HIGH-PERFORMANCE MAG-  
NETIC MATERIALS

Joseph J. Becker

General Electric Corporate Research and  
Development

Prepared for:

Air Force Materials Laboratory  
Advanced Research Projects Agency

April 1973

DISTRIBUTED BY:

**NTIS**

National Technical Information Service  
U. S. DEPARTMENT OF COMMERCE  
5285 Port Royal Road, Springfield Va. 22151

## **DISCLAIMER NOTICE**

**THIS DOCUMENT IS BEST QUALITY PRACTICABLE. THE COPY FURNISHED TO DTIC CONTAINED A SIGNIFICANT NUMBER OF PAGES WHICH DO NOT REPRODUCE LEGIBLY.**

0

AD 76018

TECHNOLOGY DEVELOPMENT FOR TRANSITION METAL-RARE EARTH HIGH-PERFORMANCE MAGNETIC MATERIALS

Contract No. F33615-70-C-1626  
Sponsored by the Advanced Research Projects Agency  
ARPA Order No. 1617, Program Code No. OD10  
Contract effective date: 30 June 1970. Expiration date: 30 June 1973

Approved for public release;  
distribution unlimited.

DDC  
APPROVED  
1970  
E

Submitted to:

Air Force Materials Laboratory, AFSC, USAF  
Project Engineer: J. C. Clson, LPE, Tel. (513) 255-4474

By:

J. J. Becker, Principal Investigator, Tel. (518) 346-8771, Ext. 6114  
GENERAL ELECTRIC COMPANY  
CORPORATE RESEARCH AND DEVELOPMENT  
P. O. Box 8  
SCHENECTADY, NEW YORK 12301

The views and conclusions contained in this document are those of the authors and should not be interpreted as necessarily representing the official policies, either expressed or implied, of the Advanced Research Projects Agency or the U. S. Government.

PHYSICAL  
SCIENCE

SRD-73-059

47

NOTICE

When Government drawings, specifications, or other data are used for any purpose other than in connection with a definitely related Government procurement operation, the United States Government thereby incurs no responsibility nor any obligation whatsoever; and the fact that the government may have formulated, furnished, or in any way supplied the said drawings, specifications, or other data, is not to be regarded by implication or otherwise as in any manner licensing the holder or any other person or corporation, or conveying any rights or permission to manufacture, use, or sell any patented invention that may in any way be related thereto.

RECEIVED IN	
NTIS	<input checked="" type="checkbox"/>
CEC	<input type="checkbox"/>
...	<input type="checkbox"/>
A	

Copies of this report should not be returned unless return is required by security considerations, contractual obligations, or notice on a specific document.

UNCLASSIFIED

Security Classification

DOCUMENT CONTROL DATA - R & D

(Security classification of title, body of abstract and indexing annotation must be entered when the overall report is classified)

1. ORIGINATING ACTIVITY (Corporate author) General Electric Company Corporate Research and Development Schenectady, New York		2a. REPORT SECURITY CLASSIFICATION Unclassified	
		2b. GROUP	
3. REPORT TITLE TECHNOLOGY DEVELOPMENT FOR TRANSITION METAL-RARE EARTH HIGH-PERFORMANCE MAGNETIC MATERIALS			
4. DESCRIPTIVE NOTES (Type of report and inclusive dates) Semiannual Interim Technical Report - 1 July 1972 to 31 December 1972			
5. AUTHOR(S) (First name, middle initial, last name) Joseph J. Becker			
6. REPORT DATE April 1973	7a. TOTAL NO. OF PAGES 31	7b. NO. OF REFS 94	
8a. CONTRACT OR GRANT NO. F33615-70-C-1626	9a. ORIGINATOR'S REPORT NUMBER(S) SRD-73-059		
b. PROJECT NO. ARPA Order No. 1617			
c. Program Code No. OD10	9b. OTHER REPORT NO(S) (Any other numbers that may be assigned this report) AFML-TR-73-50		
10. DISTRIBUTION STATEMENT Approved for public release; distribution unlimited.			
11. SUPPLEMENTARY NOTES Details of illustrations in this document may be better studied on microfiche.		12. SPONSORING MILITARY ACTIVITY Air Force Materials Laboratory (LPE) Wright-Patterson Air Force Base Ohio 45433	
13. ABSTRACT Contributions to the coercive force from expanding domain walls and from inter-phase boundaries are considered. A phenomenological model for the magnetizing field dependence of the behavior of a single particle is described. An invited session at the 1972 Magnetism Conference reviewed the coercivity problem. Theory and experiments relating to coercivity in cobalt-rare earth compounds are reviewed. Coercivity is predominantly limited by the nucleation of reverse domains by defects. Domain-wall pinning also influences coercivity in some cases. The specific defects responsible for domain nucleation have not been conclusively identified, but may be cobalt-rich regions and deformation-induced dislocations and stacking faults. Preliminary studies suggest that the high-temperature decomposition of Co <sub>5</sub> Sm takes place by a precipitation reaction rather than by eutectoidal decomposition. Attempts were made to prepare Co <sub>3</sub> R compounds with Tm, Yb, Sc, Eu, and Lu. The mechanical hardness of sintered magnets does not vary with heat treatment temperature even though the coercive force varies by a factor of twenty. Diffusion couples have been made between cobalt and a 60 wt% Sm alloy. In sintered magnets, x-ray lattice parameters, chemical composition, phase identification by metallography, and magnetic properties have been measured for a series of closely spaced compositions. The peak magnetic properties occur when the composition is close to the Co <sub>5</sub> Sm - Co <sub>7</sub> Sm <sub>2</sub> phase boundary. Changes in lattice parameter with temperature over the range 77° to 300°K are reported.			

DD FORM 1 NOV 68 1473

UNCLASSIFIED

Security Classification

UNCLASSIFIED

Security Classification

14 KEY WORDS	LINK A		LINK B		LINK C	
	ROLE	WT	ROLE	WT	ROLE	WT
Magnetic Materials Permanent Magnets Cobalt-Rare Earth Magnetism						

TECHNOLOGY DEVELOPMENT FOR TRANSITION METAL-RARE  
EARTH HIGH-PERFORMANCE MAGNETIC MATERIALS

J. J. Becker et al.

Approved for public release;  
distribution is unlimited.

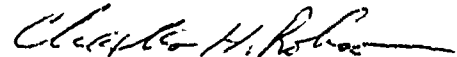
## FOREWORD

This report describes work carried out in the Metallurgy and Ceramics Laboratory of the General Electric Research and Development Center, Schenectady, New York, under USAF Contract No. F33615-70-C-1626, entitled "Technology Development for Transition Metal-Rare Earth High-Performance Magnetic Materials." This work is administered by the Air Force Materials Laboratory, Wright-Patterson Air Force Base, Ohio, J. C. Clson (AFML/LPE), Project Engineer.

This Fifth Semiannual Interim Technical Report covers work conducted under the above program during the period 1 July - 31 December 1972. The principal participants in the research are J. J. Becker, J. D. Livingston, J. G. Smeggil, D. L. Martin, M. G. Benz, and A. C. Rockwood. The report was submitted by the author in January 1973.

The contractor's report number is SRD-73-059.

This technical report has been reviewed and is approved.



CHARLES H. ROBISON

Major, USAF

Chief, Solid State Materials Branch

Materials Physics Division

Air Force Materials Laboratory



## TABLE OF CONTENTS

<u>Section</u>		<u>Page</u>
I	INTRODUCTION- - - - -	1
II	FUNDAMENTAL STUDIES OF THE ORIGIN OF THE COERCIVE FORCE IN HIGH-ANISOTROPY MATERIALS- -	1
	1. Origin of the coercive force (J. J. Becker) - - - - -	1
	2. A model for the field dependence of magnetization discontinuities in cobalt-rare-earth materials (J. J. Becker) - - - - -	3
	3. Session on origin of coercive force - - - - -	5
	4. Present understanding of coercivity (J. D. Livingston) -	5
	5. Present understanding of coercivity in cobalt-rare- earths (J. D. Livingston) - - - - -	13
III	MATERIALS CHARACTERIZATION AND PHASE EQUILIBRIUM STUDIES - - - - -	1
	1. Studies of the decomposition of $\text{Co}_5\text{Sm}$ at elevated temperatures (J. G. Smeggil) - - - - -	1
IV	ALLOY STUDIES - - - - -	1
	1. Preparation and examination of $\text{Co}_5\text{Tm}$ , $\text{Co}_5\text{Yb}$ , $\text{Co}_5\text{Sc}$ , $\text{Co}_5\text{Eu}$ , and $\text{Co}_5\text{Lu}$ (J. D. Livingston) - - - - -	1
	2. Variation of mechanical hardness and coercive force with post-sintering heat treatment (J. G. Smeggil) - - -	1
	3. Diffusion studies (D. L. Martin) - - - - -	1
	4. Cobalt-samarium permanent magnet alloys: variation of lattice parameters with composition and temperature (D. L. Martin, M. G. Benz, and A. C. Rockwood) - - - - -	5

## LIST OF ILLUSTRATIONS

<u>Section</u>	<u>Page</u>
II-4	<u>Present understanding of coercivity</u>
Fig. 1	Coercivity models and corresponding coercivities - - - 5
Fig. 2	Magnetic behavior predicted by general pinning and nucleation models - - - - - 7
Fig. 3	Dependence on defect density of nucleation and pinning models - - - - - 8
Fig. 4	Effect on coercivity of various processes, and possible cause on pinning model - - - - - 9
Fig. 5	Mechanisms determining coercivity - - - - - 10
II-5	<u>Present understanding of coercivity in cobalt-rare earths</u>
Fig. 1	a-c: Equilibrium magnetization curves for spheres of various diameters. d-f: Ideal hysteresis curves for same particles, assuming $D \gg b_c$ . Coercivity is $(2K/M_S) - N_1 M_S$ . - - - - - 1
Fig. 2	Hysteresis loop of $\text{Co}_5\text{Y}$ particle - - - - - 4
Fig. 3	Hysteresis loop of $200\mu$ $\text{Co}_5\text{Sm}$ particle - - - - - 4
Fig. 4	Hysteresis loop of $50\mu$ $\text{Co}_5\text{Sm}$ particle - - - - - 4
Fig. 5	Hysteresis loop of $5\mu$ $\text{Co}_5\text{Sm}$ particle - - - - - 4
Fig. 6	Coercivity vs annealing temperature for $\text{Co}_5\text{Sm}$ and $\text{Co}_5\text{Pr}$ . Dashed lines for as-ground specimens. Solid lines after initial anneal near $1000^\circ\text{C}$ - - - - - 5
Fig. 7	Relative coercivity vs temperature for a series of $\text{Co}_5\text{Sm}$ sintered magnets - - - - - 6
Fig. 8	Coercivity vs anisotropy constant (measured at various temperatures) for a $\text{Co}_5\text{Sm}$ sintered magnet - 6

List of Illustrations (continued)

<u>Section</u>	<u>Page</u>
III-1	Studies of the decomposition of $\text{Co}_5\text{Sm}$ at elevated temperatures
Fig. 1	$\text{Co}_5\text{Sm} + \text{Co}_7\text{Sm}_2$ . As cast. Etched with 1% nital - 5% hydrol. ----- 2
Fig. 2	$\text{Co}_5\text{Sm} + \text{Co}_7\text{Sm}_2$ . Annealed 21 days at $750^\circ\text{C}$ . Etched with 1% nital - 5% hydrol ----- 3
IV-1	Preparation and examination of $\text{Co}_5\text{Tm}$ , $\text{Co}_5\text{Yb}$ , $\text{Co}_5\text{Sc}$ , $\text{Co}_5\text{Eu}$ , and $\text{Co}_5\text{Lu}$
Fig. 1	Co-Tm as-cast ----- 2
Fig. 2	Co-Tm as-cast (domains) ----- 2
Fig. 3	Co-Sc as-cast ----- 3
Fig. 4	Co-Yb as-cast ----- 3
IV-4	Cobalt-samarium permanent magnet alloys: variation of lattice parameters with composition and temperature
Fig. 1	Change of $\text{Co}_5\text{Sm}$ lattice parameters and density with adjusted samarium content ----- 3
Fig. 2	Magnetic properties after sintering and aging as a function of the adjusted samarium content of the Co-Sm alloy phase or phases ----- 5
Fig. 3	Change of x-ray parameters with temperature for two Co-Sm samples. The $\circ$ points are for 16.8 at. % Sm sample, and the $\bullet$ points are for a 16.7 at. % Sm sample ----- 6

# TECHNOLOGY DEVELOPMENT FOR TRANSITION METAL - RARE EARTH HIGH-PERFORMANCE MAGNETIC MATERIALS

J. J. Becker

## I. INTRODUCTION

This is the fifth semiannual interim technical report for Contract No. F33615-70-C-1626, covering the period 1 July 1972 through 31 December 1972. The objective of this work, as set forth in Exhibit A of the contract, is to develop the technology of high-performance transition metal-rare earth magnets for critical applications. High-performance permanent magnets are defined in this context as those having remanences greater than ten thousand gauss and permeabilities of very nearly unity throughout the second and into the third quadrants of their hysteresis loop. Such technology is to be developed through 1) studies of the origin of the intrinsic coercive force in high-anisotropy materials, 2) development of information on phase equilibria in these materials, and 3) identification and investigation of new materials. The progress that has been made during the period covered by this report is described below under these three major headings. This report includes a digest and two papers that have been accepted for presentation or published in various technical journals.

## II. FUNDAMENTAL STUDIES OF THE ORIGIN OF THE COERCIVE FORCE IN HIGH-ANISOTROPY MATERIALS

### 1. Origin of the coercive force (J. J. Becker)

In the continuing theoretical study of the origin of the coercive force in both powders and sintered magnets, a number of points are being developed. One is an assessment of the importance of changes in wall area. In an approximately equiaxed, nearly saturated particle, such as a particle at remanence having a coercive force greater than about  $4\pi M_s/3$ , any remaining vestigial domain boundary that might serve as a nucleus for magnetization reversal will necessarily greatly increase its area as it moves. This fact contributes an additional term to the total energy, with the result that the force on the wall due to a given external field depends on the overall magnetization. This factor, neglected in the usual kinds of wall-motion calculations, may be of dominating importance in the nucleated-reversal type of behavior characteristically shown by cobalt-rare earths.

A consideration that may be of importance to sintered materials as well as in particles is the barrier to wall motion presented by a boundary between two crystallographic phases. Such boundaries may be considered to exist in the "shell" model for sintered magnets, in which each grain of the 5-1 phase

is hypothesized to be surrounded by a layer of 7-2. They would also exist at isolated nuclei such as those provided by local oxidation resulting in a bit of high-cobalt low-anisotropy material. While the magnetization could easily rotate in such a nucleus, the resulting domain wall must then cross the boundary into the 5-1 phase. Depending on the spatial orientation of the boundary in this type of situation, the domain wall energy may have to increase substantially over a distance on the same order as its own thickness. This can lead to very large coercive forces. In the case of the shell model, granting the hypothetical shell of 7-2 phase, the presence of the phase boundary seems like a simpler physical origin for the coercive force than the further hypothesis that the 7-2 phase is full of pinning sites.

A phenomenological treatment of the dependence of  $H_n$  on  $H_m$  for single particles is being developed along the lines that are summarized in the following digest, which has been accepted for presentation at the 1973 Intermag Conference.

2. A MODEL FOR THE FIELD DEPENDENCE OF MAGNETIZATION  
DISCONTINUITIES IN COBALT-RARE-EARTH MATERIALS

J. J. Becker

(To be presented at the 1973 Intermag Conference)

# A MODEL FOR THE FIELD DEPENDENCE OF MAGNETIZATION DISCONTINUITIES IN COBALT-RARE-EARTH MATERIALS

J. J. Becker

General Electric Research and Development Center  
P. O. Box 8, Schenectady, New York 12301

A strong dependence of intrinsic coercive force  $H_c$  on previous magnetizing field  $H_m$  has been observed in powders of cobalt-rare-earths. Observations on  $\text{Co}_5\text{Sm}$  single particles<sup>(1)</sup> demonstrate that the fields  $H_n$  at which magnetization discontinuities take place also vary with  $H_m$ , showing that the dependence is a property of each particle. In general the values of  $H_m$  are larger than  $H_n$ , and the overall slope of  $H_n$  as a function of  $H_m$  is approximately -1, until a value of  $H_m$  is reached that results in no further increase of  $H_n$ .

It is possible to explain this type of behavior on a simple phenomenological model. The essential features of the model are the following:

1. The particle contains sites that trap small pieces of domain wall. There is an energy barrier for the wall to leave the trap, taken for simplicity as the same in either direction of motion.
2. The event that brings about a discontinuous magnetization jump is the breaking away of a wall fragment from its trap. This occurs at a local field  $-H_d$ . The corresponding applied field  $H_n$  is equal to  $H_d - H_d$ , where  $H_d$  is the local demagnetizing field. Thus  $H_n$  may be positive or negative.
3. The wall fragment may equally well be driven in the other direction, removing the small remaining domain and slightly increasing the magnetization in the direction of the applied field. This will happen at a local field  $+H_d$ , or an applied field  $H_d + H_d$ .
4. Once the wall has been driven out of the trap, in either direction, the trap has been inactivated and will do nothing further until it captures another bit of wall. This will happen when another trap "fires."
5. Ultimately at high  $H_m$  another type of defect takes over and determines the limiting value of  $H_n$ .

This model predicts the following types of behavior:

1. Loops at less than the limiting  $H_m$  are characteristically unsymmetrical, since they are due to two traps, one reactivating the other.
2. At the limiting  $H_m$  the loop becomes symmetrical.

3. The predicted behavior of  $H_n$  as a function of  $H_m$  has an overall slope of -1 and an offset of  $H_d$ . That is, no jumps take place until  $H_m$  exceeds  $H_d$ .

Comparison of these predictions with the observed behavior of a particle whose ideal loops at the limiting  $H_m$  have been reported previously<sup>(2)</sup> indicates the presence of several such defects in addition to the limiting one and shows a reasonable value of about 2400 Oe for  $H_d$ .

1. J.J. Becker, IEEE Trans. Magnetics MAG-5, 211 (1969).
2. J.J. Becker, J. Appl. Phys. 42, 1537 (1971).

---

This research was supported by the Advanced Research Projects Agency of the Department of Defense and was monitored by the Air Force Materials Laboratory, MAYE, under Contract F33615-70-1626.



### 3. Session on Origin of Coercive Force

During the time of the present report, the author organized and chaired a session on the origin of the coercive force in high-anisotropy materials, the Symposium-Workshop on Cobalt-Rare-Earths, held at the 18th Annual Conference on Magnetism and Magnetic Materials in November. The session consisted of a paper reviewing the present status of the problem, given by J. D. Livingston, followed by a panel discussion. The panel members included K. J. Strnat, University of Dayton; R. A. McCurrie, University of Bradford, England; K. Bachmann, Brown-Boveri, Switzerland; and G. Y. Chin, Bell Laboratories. The purpose of the session was to pinpoint as precisely as possible where the understanding of the problem stands, what discrepancies exist, and what exactly should be done next to advance the understanding of this subject most effectively, thereby establishing the strongest possible base for continued development of this class of materials. The size of the audience and the degree of its participation throughout the session were most gratifying and amply testified to the widespread interest in this important subject.

A precis of the oral presentation of the review paper is given next, followed by the text of the written version. This is done because for the oral version several additional slides were prepared to present the material in somewhat simpler form. These figures and the comments on them are included here for the pedagogical value they may have.

### 4. Present understanding of coercivity (J. D. Livingston)

Figure 1 shows the various coercivity models so far suggested for high-anisotropy uniaxial materials such as  $\text{Co}_5\text{Sm}$ . Coherent rotation and curling can be eliminated because the experimentally observed coercivities are much lower than the theoretical values for these reversal processes. Thus we conclude that reversal occurs by the nucleation and growth of reverse domains. Coercivity is controlled either by the nucleation event, by general wall pinning, or, according to models developed by Zijlstra, Westorp, and Strnat and co-workers, by a localized wall-pinning.

Figure 2 shows schematically the different magnetic behavior predicted by general pinning and nucleation models. The behavior at the top, characteristic of general pinning, is observed for copper-bearing precipitation alloys. The behavior at the bottom, on the other hand, is characteristic of predominantly single-phase  $\text{Co}_5\text{R}$  materials. This observation rules out general pinning in these cases, and is consistent with nucleation-controlled reversal. However, certain local pinning models can also explain such behavior.

Study of the magnetization curves of individual  $\text{Co}_5\text{R}$  particles (Figs. 2-5 in the next section) shows that both nucleation and local pinning can play a




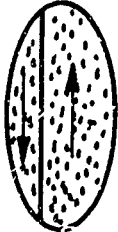
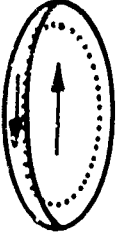
<u>MODEL</u>	<u>COERCIVITY</u>
	$\frac{2K}{M_s} + (N_{\perp} - N_{\parallel})M_s$
	$\frac{2K}{M_s} - N_{\parallel} M_s$
	$H_{\text{nucl}}$
	$H_{\text{unpin}}$
	$H_{\text{unpin}}$

Figure 1 Coercivity models and corresponding coercivities.

## GENERAL PINNING



## NUCLEATION (and local pinning?)

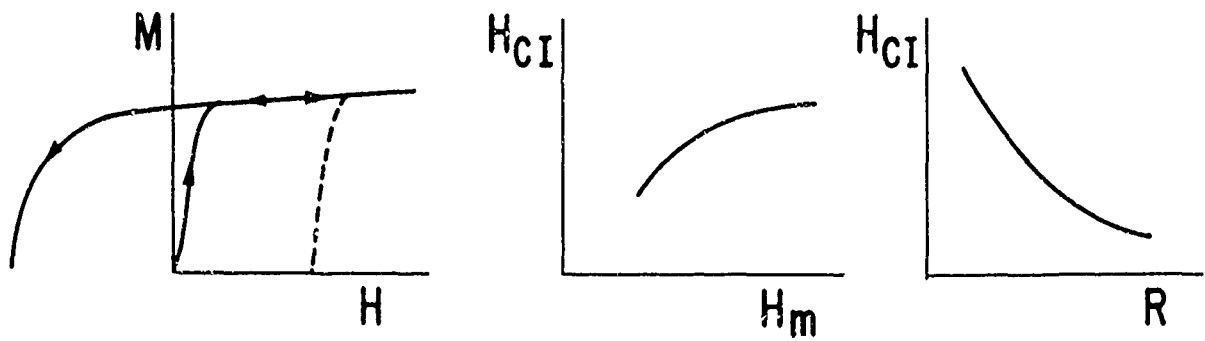


Figure 2 Magnetic behavior predicted by general pinning and nucleation models.

NUCLEATION

Defects

lower  $H_{CI}$

PINNING

Defects

raise  $H_{CI}$

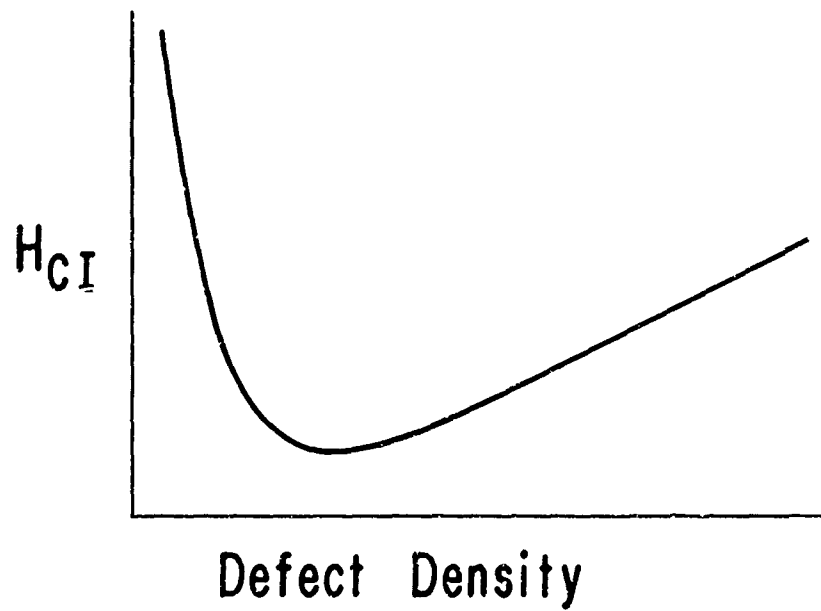


Figure 3 Dependence on defect density of nucleation and pinning models.






<u>PROCESS</u>	<u>EFFECT ON <math>H_{CI}</math></u>	<u>POSSIBLE CAUSE</u>
GRINDING		PARTICLE SIZE, DISLOCATIONS
AGING (OXIDATION)		COBALT-RICH REGIONS
ETCHING		REMOVAL OF SURFACE DEFECTS
ANNEALING NEAR 1000°C		REMOVAL OF DEFECTS
ANNEALING NEAR 700°C		PRECIPITATES

Figure 4 Effect on coercivity of various processes, and possible cause on pinning model.

## MECHANISMS DETERMINING COERCIVITY

Precipitation Alloys  
(Co - Cu - Fe - R)

GENERAL WALL  
PINNING

Co<sub>5</sub>R Single Particles

NUCLEATION &  
LOCAL PINNING

Powders  
Sintered Magnets

} NUCLEATION  
( & LOCAL PINNING ? )

Figure 5 Mechanisms determining coercivity.

role in controlling coercivity. Considered in detail, the models in fact can be difficult to distinguish in some respects. However, as shown schematically in Fig. 3, the two models involve opposite dependences on defect density. The curve shows that a few defects can lower coercivity by nucleation of reverse domains, but a sufficiently high density of defects can raise coercivity through wall pinning. Therefore, in principle, to establish whether nucleation or local pinning is dominating coercivity in powder assemblies or sintered magnets, we need only determine whether coercivity is increasing or decreasing with increasing defect density. In practice, interpretation is somewhat ambiguous because the nature of the important defects, and their connection with various processing steps, are generally unestablished.

Figure 4 shows schematically the effect on coercivity of various processes such as grinding, low-temperature aging, etc., and a possible explanation for a pinning-controlled model. For example, the increase of coercivity on etching has been attributed to an introduction of pinning centers, perhaps due to hydrogen, by the etching process. The explanation based on nucleation seems more plausible in view of our general knowledge of defects, but more metallographic studies are needed to establish definitively the significant defects and their density after various processing steps.

Finally, Fig. 5 summarizes the conclusions reached in the above discussion.

5. Present Understanding of Coercivity in Cobalt-Rare-Earths

J. D. Livingston

(To be published in AIP Conference Proceedings)



**GENERAL  ELECTRIC**

**GENERAL ELECTRIC COMPANY  
CORPORATE RESEARCH AND DEVELOPMENT**

**Schenectady, N.Y.**

---

---

---

---

---

---

**PRESENT UNDERSTANDING OF COERCIVITY IN  
COBALT-RARE EARTHS**

by

**J. D. Livingston  
Metallurgy and Ceramics Laboratory**

Report No. 72CRD316

November 1972

---

---

---

---

---

---

**TECHNICAL INFORMATION SERIES**

**CLASS 1**

*22*

General Electric Company  
Corporate Research and Development  
Schenectady, New York

AUTHOR Livingston, JD	SUBJECT permanent magnets	NO 72CRD316
TITLE Present Understanding of Coercivity in Cobalt-Rare Earths		DATE November 1972
ORIGINATING COMPONENT Metallurgy and Ceramics Laboratory		GE CLASS 1
		NO PAGES 9
<p><b>SUMMARY</b></p> <p>Theory and experiments relating to coercivity in cobalt-rare earth compounds are reviewed. Coercivity is predominantly limited by the nucleation of reverse domains by defects. Domain-wall pinning also influences coercivity in some cases. The specific defects responsible for domain nucleation have not been conclusively identified, but may be cobalt-rich regions and deformation-induced dislocations and stacking faults. This review was prepared for a symposium-workshop at the 1972 Conference on Magnetism and Magnetic Materials.</p>		
<p><b>KEY WORDS</b></p> <p>permanent magnets, coercivity, cobalt-rare earth compounds</p>		

INFORMATION PREPARED FOR \_\_\_\_\_

Additional Hard Copies Available From

Corporate Research & Development Distribution  
P.O. Box 43 Bldg. 5, Schenectady, N.Y., 12301

Microfiche Copies Available From

Technical Information Exchange  
P.O. Box 43 Bldg. 5, Schenectady, N.Y., 12301

PRESENT UNDERSTANDING OF COERCIVITY IN COBALT-RARE EARTHS

J. D. Livingston

INTRODUCTION

Co<sub>5</sub>Sm and Co<sub>5</sub>Sm-based ternary compounds have recently been developed into permanent magnets with energy products and coercivities substantially greater than was possible with previous materials.<sup>(1-3)</sup> However, in other Co<sub>5</sub>R, Co<sub>17</sub>R<sub>2</sub>, and (Co, Fe)<sub>17</sub>R<sub>2</sub> compounds with the potential for higher energy products and/or lower material costs than Co<sub>5</sub>Sm, high coercivities have not yet been achieved. Even in Co<sub>5</sub>Sm, coercivities remain almost an order of magnitude below those theoretically possible. Thus there remains considerable technological potential in improved understanding of the factors determining coercivity in these materials.

The Co<sub>5</sub>R compounds are of hexagonal symmetry, and the basis for large coercivities is the large, easy-axis, magnetocrystalline anisotropy which has been measured on single crystals<sup>(4-6)</sup> and aligned powders<sup>(5, 7)</sup>. We will review first the theory of magnetization reversal in easy-axis materials, and then the experiments relating to coercivity in the cobalt-rare earths. We will deal exclusively with the intrinsic coercivity H<sub>ci</sub>, the reverse field in which half of the specimen magnetization is reversed. Unless otherwise specified, we will be considering the case in which magnetic field is applied parallel to the easy axis.

THEORY

Critical Particle Sizes

There are three different size parameters of significance to single-domain behavior.<sup>(8)</sup> These are D<sub>c</sub> = 1.4γ/M<sub>s</sub><sup>2</sup>, b<sub>c</sub> = 2A<sup>2</sup>/M<sub>s</sub>, and δ = π(A/K)<sup>2</sup>, where M<sub>s</sub> is saturation magnetization, K is magnetocrystalline anisotropy, A is the exchange constant and γ = 4(AK)<sup>2</sup> is the domain-wall energy per unit area.

The first parameter, D<sub>c</sub>, is the diameter of a sphere below which a single-domain structure is of lower energy at zero field than a multidomain structure. The dimension b<sub>c</sub> is the cylinder diameter below which magnetization reversal by coherent rotation is favored over the incoherent curling process. The third parameter, δ, is the width of a domain wall.

The three parameters are related through b<sub>c</sub> ≈ ½(D<sub>c</sub>δ)<sup>½</sup>. The ratio D<sub>c</sub>/b<sub>c</sub> = K/M<sub>s</sub><sup>2</sup> is a measure of the relative importance of crystal and shape anisotropies. In most Co<sub>5</sub>R compounds, crystal anisotropy dominates, i. e., K >> M<sub>s</sub><sup>2</sup>. The various size parameters for these compounds are typically D<sub>c</sub> ≈ 1μ, b<sub>c</sub> ≈ 400 Å, and δ ≈ 60 Å. In contrast, in pure cobalt, all three size parameters are of the same order of magnitude, about 150 Å to 300 Å. In iron and nickel, D<sub>c</sub> < b<sub>c</sub>.

We consider first the equilibrium or lowest-energy magnetization states of a uniaxial particle temporarily ignoring the accessibility of those states. The equilibrium magnetization curves for spherical particles with D ≤ D<sub>c</sub>, D ≥ D<sub>c</sub>, and D >> D<sub>c</sub> are shown in the top half of Fig. 1. For D ≤ D<sub>c</sub>, the particle is always fully saturated, i. e., single domain, in its lowest-energy state. For a bulk sphere (D >> D<sub>c</sub>), a multidomain state with zero internal field is of lowest energy for applied fields below the saturating field of 4πM<sub>s</sub>/3. For intermediate particle sizes, the field range over which the multidomain state is favored decreases with decreasing diameter, with the fractional decrease in saturating field varying approximately as (D<sub>c</sub>/D)<sup>2/3</sup>. Thus the transition from multidomain behavior to single-domain behavior is gradual, and does not occur abruptly at D = D<sub>c</sub>.

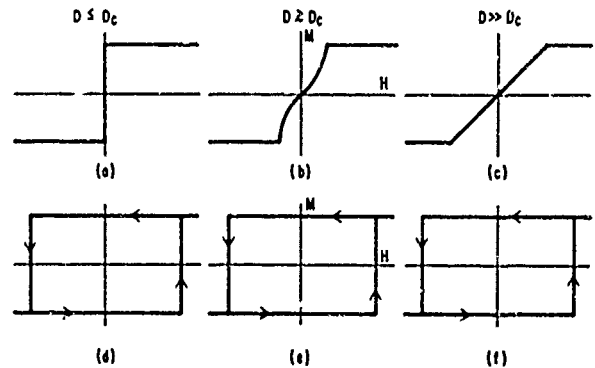


Fig. 1 (a)-(c): Equilibrium magnetization curves for spheres of various diameters. (d)-(f): Ideal hysteresis curves for same particles, assuming D >> b<sub>c</sub>. Coercivity is (2K/M<sub>s</sub>) - N<sub>1</sub>M<sub>s</sub>.

These equilibrium curves correspond to lowest-energy states, and it is the energy barriers between these states that lead to hysteresis and coercive force. In particular, micromagnetic theory<sup>(10)</sup> indicates that a fully saturated magnetization state is very stable. For a saturated, defect-free ellipsoid of rotation with D < b<sub>c</sub>, the second size parameter, this theory predicts that magnetization reversal cannot be nucleated until the application of a reverse field -H<sub>11</sub> = 2K/M<sub>s</sub> + (N<sub>2</sub> - N<sub>1</sub>)M<sub>s</sub>, where N<sub>1</sub> and N<sub>2</sub> are the longitudinal and transverse demagnetizing factors. This field corresponds to the coercivity for coherent rotation, i. e., Stoner-Wohlfarth<sup>(11)</sup> behavior. For D > b<sub>c</sub>, nucleation can occur via the curling mode at a lower field, which approaches 2K/M<sub>s</sub> - N<sub>1</sub>M<sub>s</sub> for D >> b<sub>c</sub>. For materials for which K > M<sub>s</sub><sup>2</sup>, such as Co<sub>5</sub>Sm, this decreases in nucleating field provided by curling is minor. The magnetization curves predicted by micromagnetic theory for defect-free particles are shown in the bottom half of Fig. 1. For D >> b<sub>c</sub>, the predicted coercivity is size-independent (Brown's paradox).

For any real particle, the magnetization curve for each size range must fall between the two limiting curves at the top and bottom of Fig. 1, i. e., between equilibrium and ideally hysteretic behavior. Defects play two contrary roles in determining where the real particle's magnetization curve will fall. On the one hand, they can provide sites for heterogeneous nucleation of magnetization reversal, and thereby aid the approach to equilibrium. On the other hand, they can inhibit the motion of domain walls, and thereby oppose the approach to equilibrium. Through these two effects--nucleation and pinning--defects can therefore either decrease or increase coercivity.

### Heterogeneous Domain Nucleation

The maximum room-temperature  $H_{ci}$  produced to date with  $\text{Co}_2\text{Sm}$  is 43 kOe,<sup>(12)</sup> about one-seventh of  $2K/M_s$ , the ultimate coercivity predicted by theory ( $N_1 = 0$ ). Most magnets and powders have coercivities considerably smaller. Since coherent rotation and curling are impossible at such low fields, it appears likely that reverse domains are being nucleated at defects.

One possible cause for nucleation is high local demagnetizing fields at surface irregularities (sharp corners or pits)<sup>(13-15)</sup> or inclusions.<sup>(16)</sup> Although the demagnetizing field at a mathematically sharp corner is infinite,<sup>(13)</sup> Aharoni noted that a radius less than atomic dimensions is unrealistic, and for realistic dimensions the maximum local demagnetizing field possible is about  $18M_s$ .<sup>(17)</sup> When  $K \gg M_s^2$ , these maximum demagnetizing fields are much smaller than  $2K/M_s$ , and therefore cannot directly explain the low coercivities observed. However, these sites will require magnetizing fields above  $18M_s$ , e. g., about 15 kOe for  $\text{Co}_2\text{Sm}$ , to remove residual reverse domains and produce initial saturation.

Another possible nucleation site is a local region in which  $K$  is appreciably lowered. In  $\text{Co-R}$  magnets, this could correspond to a cobalt-rich region produced, for example, by preferential oxidation of the rare earth. Local elastic strains, e. g., around a dislocation, could also decrease  $K$ , although magnetostrictive constants would have to be unusually high to reduce  $K$  to near zero in a high-anisotropy material such as  $\text{Co}_2\text{Sm}$ . Abraham and Aharoni<sup>(18)</sup> calculated the reduction in nucleation field produced by a cylinder or slab of material with  $K$  0 lying parallel to the field. The reduction is substantial once the cylinder diameter or slab thickness becomes larger than  $\lambda$ , the domain-wall width. For defects smaller than  $\lambda$ , exchange forces are sufficient to resist reversal by this mechanism.

Another possible nucleation site in ordered magnetic crystals is a stacking fault. Magnetic coupling in some structures can be greatly altered across a fault, and may even be antiferromagnetic.<sup>(15, 16)</sup> Such a fault may be an easy nucleation source for a  $180^\circ$  domain wall.

Even after a small reverse domain has been formed at a defect, the domain-wall surface energy  $\gamma$  can resist its expansion.<sup>(20, 21)</sup> For example, calculations for plane domains in spherical particles<sup>(22)</sup> and cylindrical domains in plates<sup>(9)</sup> show an energy barrier opposing domain growth until the domain reaches a critical breakaway size. The calculated size decreases with increasing field, and perhaps breakaway can first occur when this size equals the size of the defect. For the case of a cylindrical domain in a plate of thickness  $T$ , a domain nucleated at a defect of size  $\Delta$  would then break away at a field of  $-H_H = (\gamma/2M_s\Delta) + (32M_s\Delta/T) - 4\gamma M_s$ . The first term represents the resistance to breakaway provided by wall energy. For  $\text{Co}_2\text{Sm}$  and  $\Delta = 500\text{\AA}$ , this term is about 10 kOe.

The likelihood of a particle containing a defect capable of nucleating a reverse domain is expected to decrease with decreasing particle size. Thus when nucleation controls coercivity, coercivity increases as particle size decreases. Attempts to explain the experimentally observed variations of coercivity with size have been made from domain models using arbitrary assumptions about the size or height of energy barriers that can be overcome<sup>(22)</sup> or models based on the statistical probability of effective nuclei in particles of a given size.<sup>(10)</sup>

### Domain-Wall Pinning

Local variations in magnetic properties can produce local variations in domain-wall energy and thereby produce forces that resist wall motion. Non-magnetic inclusions, for example, produce an attractive force because of a reduction in both wall energy and demagnetizing energy. The former is more important for inclusions smaller than  $D_c$  in diameter. If the pinning centers are few and widely spaced, the wall is presumed to bow between pins, and theory predicts an intrinsic coercivity proportional to  $\gamma/M_s\lambda$ , where  $\lambda$  is the spacing between pins.<sup>(23)</sup> If the density of pinning centers becomes high, the problem becomes much more complex, and coercivity is no longer proportional to  $\gamma$ .<sup>(24)</sup>

Zijlstra<sup>(23)</sup> and Westendorp<sup>(25)</sup> suggested a model in which pinning centers do not exist throughout a particle, but only within a surface layer. Possible pinning centers include inclusions, dislocations, stacking faults, and surface irregularities. If nucleation sites for reverse domains also exist within this layer, then these pinning centers, although only local can limit the expansion of the reverse domains and thereby influence coercivity. If these pinning centers are limited only to the immediate vicinity of the nucleation site, this model becomes difficult to distinguish from a nucleation model. A local region of closely spaced pinning sites or a stacking fault<sup>(26)</sup> could also serve to retain a residual reverse domain to high magnetizing fields, and thereby create a subsequent nucleation site.

It has recently been suggested that in some materials with large values of the ratio  $K/A$  the domain wall may be thinner than predicted by the standard expression for  $\delta$ .<sup>(27)</sup> These narrow walls may produce an intrinsic lattice resistance to domain wall motion analogous to the Peierls force that resist conlocation motion. This will probably provide little wall coercivity at room temperature, but the narrow-wall structure may alter  $\gamma$  and its dependence on  $K$  and  $A$ .

### Particle Interaction

When an assembly of particles is aligned and sintered into a dense compact, it is no longer reasonable to consider the particles as fully independent. At the very least, each grain will have strong magnetostatic interaction with neighboring grains. The reversal of neighbors along the field direction will produce extra fields tending to reverse a grain's magnetization, whereas the reversal of neighbors in the direction transverse to the field will produce the opposite effect. The most extreme case will be the field on a transverse plane of unreversed particles if the entire remainder of the sample is reversed. This will produce a field of  $8\pi M_s$  tending to reverse the magnetization of that plane. If a single spherical grain remains unreversed, the reversing field will be  $8\pi M_s/3$ . Unaligned grains will have more complex effects.

If sintering produces actual exchange contact between spins in neighboring grains, magnetization reversal can proceed directly from grain to grain by wall motion unless the boundaries provide sufficient pinning sites. Possible pinning sites are dislocations, voids, and oxide particles. It is also possible that exchange contact between the grains is blocked by a thin layer, perhaps of oxide, or greatly weakened because of atomic disorder in the boundary. Then each grain can be viewed as requiring a separate nucleation event to produce reversal. The results of Craik<sup>(28)</sup> suggest the existence of an effective gap between grains in oriented barium ferrite.

## EXPERIMENT

### Precipitation Alloys

Nesbitt et al.<sup>(29)</sup> have studied the magnetic behavior of a single crystal of Co-Fe-Cu-Ce alloy heat treated to produce a dispersion of very fine precipitates within a  $\text{Co}_2\text{Ce}$ -rich matrix. In a thermally demagnetized specimen, they found little magnetization change at fields below the coercive field, and a very abrupt increase to near saturation at the coercive field. Since such a specimen contained many domains, this behavior is characteristic not of nucleation, but of general wall pinning. Other evidence indicating general wall pinning was a lack of dependence of coercivity on magnetizing field, and the ability to achieve high coercivity in a bulk crystal. Magnetic viscosity has also been reported.<sup>(79, 80)</sup>

### Single Particles

The magnetic behavior of predominantly single-phase Co-R materials is contrary to that for the pre-

phase Co-R materials is contrary to that for the precipitation alloys. A thermally demagnetized sample can be magnetized to near saturation in low fields, coercivity generally increases with increasing magnetizing field, and high coercivities are attained only in fine particles or sintered assemblies of particles (Refs. 3, 25, 30, 31). These characteristics indicate that general wall pinning is low and suggest that coercivity is dominated by domain nucleation. Direct magnetization studies of single particles of other uniaxial hard magnetic materials, such as orthoferrites (Refs. 32-34),  $\text{MnB}$ ,<sup>(35)</sup> and  $\text{MnGa}$ ,<sup>(36)</sup> show that nucleation determines coercivity in these materials. However, the results of similar studies on single fine particles of Co-R compounds are more complex. While confirming the importance of domain nucleation, they indicate that local wall pinning can influence coercivity in some cases.

Consider the experimental magnetization curves in Figs. 2 through 5. The particle in Fig. 2 shows simple rectangular-loop behavior, similar to the bottom of Fig. 1, but with a much smaller coercivity (Ref. 37). In this particle, once the reverse domain was nucleated, it swept through and completely reversed the particle magnetization. The nucleation field and coercivity were identical. In Fig. 3, a domain nucleated and moved abruptly to a near-equilibrium position.<sup>(38)</sup> It then moved to maintain zero internal field, approximating the equilibrium behavior of Fig. 1(c), but modified by a slight wall coercivity.

However, the behavior of the particles in Figs. 4 and 5 is not so clearcut. The first shows two distinct magnetization discontinuities separated by a region of gradual change. Becker<sup>(33)</sup> interpreted this as the sum of two magnetization loops, one similar to Fig. 2 and one similar to Fig. 3 (but with nucleation at a negative applied field). He suggested that a small-angle boundary divided the particle into two magnetically independent regions. The particle in Fig. 5 shows an extensive region of gradual magnetization change, presumably corresponding to gradual wall motion, before the occurrence of a jump. Zijlstra<sup>(23, 26)</sup> interpreted this as wall motion inhibited by pinning in parts of the crystal, but not in other parts. The minor loops shown for demagnetized particles confirm that wall motion is easy over large portions of the particle.

In Figs. 2 and 3, the nucleation of one reverse domain was sufficient to reverse the particle magnetization or reach approximately equilibrium behavior. In Figs. 4 and 5, however, the nucleation of one reverse domain was insufficient, and a single barrier to wall motion or a region of pinning strongly influenced magnetization reversal.

The relative importance of domain nucleation and local wall pinning varies greatly from particle to particle, and the properties of various powders and sintered magnets may be influenced by both. Pragmatically, the goal is to increase coercivity. A nucleation-dominated model suggests we want to decrease defect density, whereas a pinning-dominated

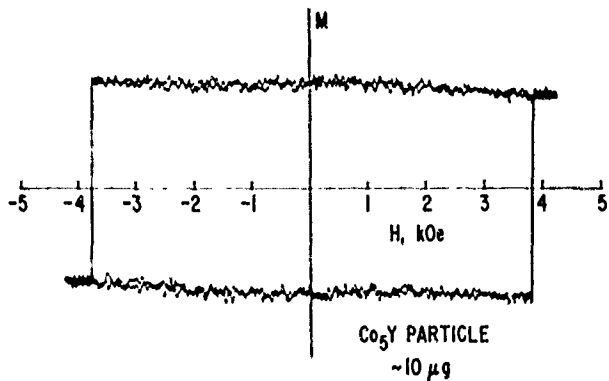


Fig. 2 Hysteresis loop of  $\text{Co}_5\text{Y}$  particle [from Becker<sup>(37)</sup>].

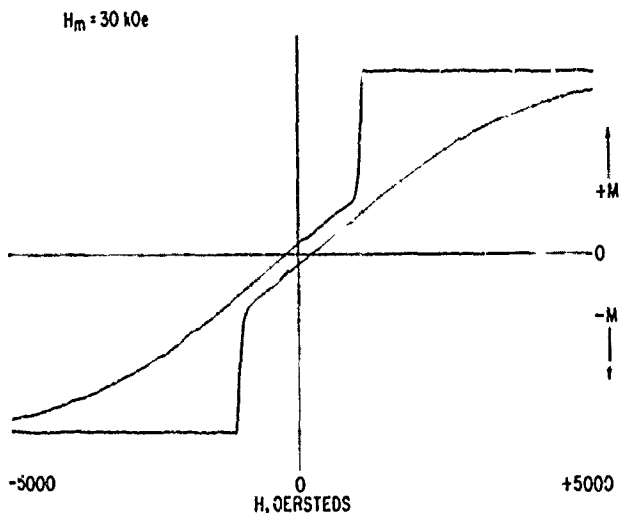


Fig. 3 Hysteresis loop of  $200\mu\text{Co}_5\text{Sm}$  particle [from Becker<sup>(38)</sup>].

model suggests we want to increase defect density. Most evidence points to the former alternative. However, incomplete evidence of the nature of the important defects and their connection with processing variables sometimes makes interpretation ambiguous.

Single-particle experiments have shown that increasing magnetizing field increases the reverse field necessary for domain nucleation in a stepwise way (Ref. 39). This suggests that residual domains, maintained by local demagnetizing fields or local pinning, are serving as reversal nuclei, and require specific magnetizing fields to remove them. Similar observations have been made on orthoferrite crystals.<sup>(32-34)</sup> Because of their low magnetization, orthoferrites have a very large  $D_c$ , and single-domains behavior is approached with dimensions of several mm. This allows direct optical observation of domain throughout the hysteresis loops. Nucleation of domains is seen to occur at specific locations in the crystal, sometimes identifiable as the location of a residual domain. When the magnetizing field is sufficiently

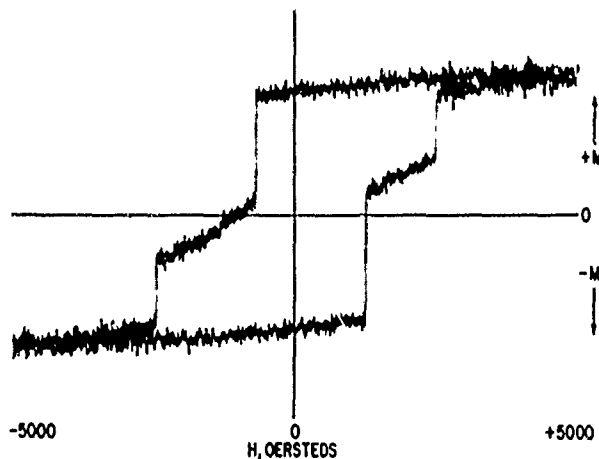


Fig. 4 Hysteresis loop of  $50\mu\text{Co}_5\text{Sm}$  particle [from Becker<sup>(38)</sup>].

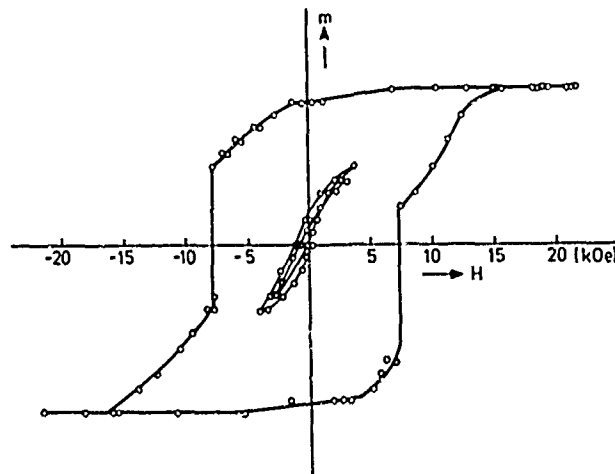


Fig. 5 Hysteresis loop of  $5\mu\text{Co}_5\text{Sm}$  particle [from Zijlstra<sup>(23)</sup>].

large to remove the residual domain, nucleation occurs at another location at a larger field. It was found that mechanical polishing made nucleation easier and annealing made it more difficult, suggesting dislocations as favored sites for magnetization reversals.<sup>(34, 40)</sup>

If individual magnetization discontinuities in a single particle can be associated with individual defects, the dependence of the nucleation fields on variables such as temperature or field orientation may shed light on the nature of the defects. Becker has reported that two such fields in one particle had different temperature dependences.<sup>(41)</sup> The  $1/\cos\theta$  dependence of coercivity expected for  $180^\circ$  domain-wall motion<sup>(42)</sup> was found displaced from  $\theta=0$  in some particles, suggesting a misoriented region as the defect site.<sup>(43)</sup>

## Powders

Coercivity of  $\text{Co}_5\text{R}$  powders first increases and then decreases with increasing grinding time, i. e., with decreasing particle size.<sup>(3, 5, 7, 30, 81)</sup> The decrease for fine sizes is usually ascribed to the plastic deformation produced by grinding. Consistent with this interpretation are the higher coercivities obtained by grinding at liquid nitrogen temperature (Refs. 7, 44, 45, 32).

McCurrie et al.<sup>(46)</sup> have observed a difference in mechanical hardness behavior between  $\text{Co}_5\text{La}$  and  $\text{Co}_5\text{Sm}$ . They conclude that plastic deformation will occur less easily in  $\text{Co}_5\text{Sm}$ , and suggest that may explain why higher coercivities are attained in that compound. A difficulty with this explanation is that  $\text{Co}_5\text{Ce}$  has similar hardness properties to  $\text{Co}_5\text{Sm}$ , but has low coercivities in ground powder, like  $\text{Co}_5\text{La}$  (Ref. 47).

Etching ground particles in various chemical reagents usually increases the coercivity, sometimes as much as twenty-fold.<sup>(3, 37, 48, 83)</sup> This may be caused by the removal of mechanically damaged surface layers, in which dislocations and stacking faults had been serving as nucleation sites. However, etching has also been observed to decrease coercive force in some cases, which was explained by the removal of a surface pinning layer.<sup>(23)</sup>

With long holding times at room temperature or slightly elevated temperatures, the coercivity of powders gradually drops,<sup>(30, 48, 80)</sup> an effect that depends on contact with oxygen<sup>(49)</sup> and can be avoided or slowed by appropriately coating the particle.<sup>(48, 50, 82, 83)</sup> This aging phenomenon may be caused by the creation of low-K cobalt-rich surface regions by preferential oxidation of the rare earth.

As mentioned earlier, thermally demagnetized  $\text{Co}_5\text{R}$  powders can be magnetized to near saturation in low fields, indicating that general wall pinning is low. Coercivity is sensitive to magnetizing field, indicating that nucleation from residual domains is controlling coercivity. Becker studied the angular dependence of the dependence of coercivity on magnetizing field, and found it consistent with a model based on the motion of  $180^\circ$  domain walls and particular assumed distributions of individual particle coercivities.<sup>(51)</sup> McCurrie<sup>(52, 53)</sup> has used demagnetizing remanence curves as a means of estimating coercivity distributions, a technique that depends on questionable assumptions about the shape of the magnetization curves of individual particles.

Zijlstra<sup>(23)</sup> measured minor loops at various positions along the reversal portion of the major hysteresis loop, and noted a nonzero susceptibility  $\chi$  which seemed likely to be caused by reversible displacements of domain walls. He then noted that  $\chi$  and coercivity  $H_{c1}$  varied with heat treatment of the powders such that  $\chi H_{c1}^2$  remained constant. He explained this correlation with a wall-pinning model. This interesting result calls for further investigation.

Annealing at temperatures near  $1000^\circ\text{C}$  can increase coercivity, perhaps because of the annealing of defects produced by grinding. However, annealing of  $\text{Co}_5\text{Sm}$  in the vicinity of  $700^\circ\text{C}$  can substantially reduce coercivity, an effect that can be reversed by a subsequent anneal at  $1000^\circ\text{C}$  (Fig. 6). Recent evidence indicates that the deleterious effect of intermediate-temperature heat treatments may be caused by a eutectoidal decomposition of  $\text{Co}_5\text{Sm}$  into  $\text{Co}_{17}\text{Sm}_2$  and  $\text{Co}_7\text{Sm}_2$ , thereby producing nuclei for easy magnetization reversal.<sup>(54, 55)</sup>

Westendorp noted a similar dependence of coercivity on heat treatment for  $\text{Co}_5\text{Pr}$ , but noted that coercivity always remained about five times smaller than for  $\text{Co}_5\text{Sm}$  (Fig. 6).<sup>(56)</sup> From domain-width observations, he concluded that the domain-wall energy for  $\text{Co}_5\text{Sm}$  was larger than for other  $\text{Co}_5\text{R}$  compounds, and suggested that the resulting increased wall-pinning forces might explain the higher coercivities of  $\text{Co}_5\text{Sm}$ . More detailed measurements have recently confirmed that the wall energy of  $\text{Co}_5\text{Sm}$  is higher than for the other compounds.<sup>(57)</sup> It was noted that this also leads to higher values of  $D_c$ , so that to grind the other compounds to an equivalent  $D/D_c$  requires finer particle sizes and therefore more mechanical damage and oxidation. This was suggested

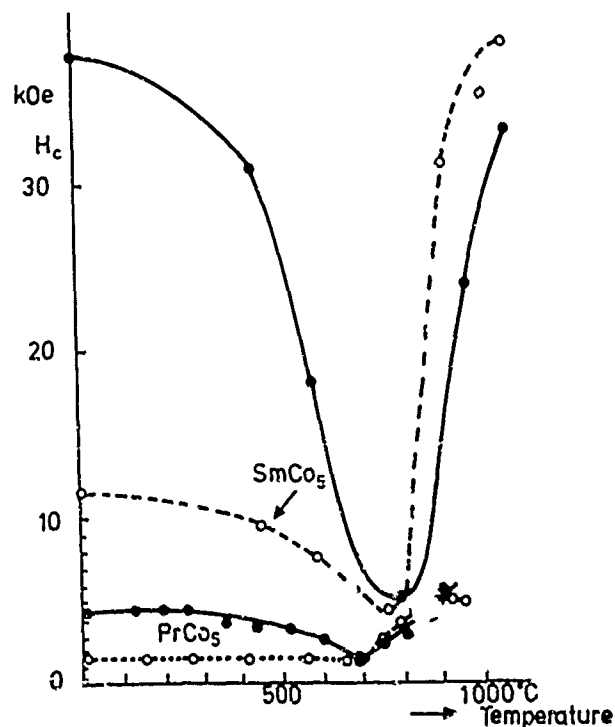


Fig. 6 Coercivity vs annealing temperature for  $\text{Co}_5\text{Sm}$  and  $\text{Co}_5\text{Pr}$ . Dashed lines for as-ground specimens. Solid lines after initial anneal near  $1000^\circ\text{C}$  [from Westendorp<sup>(56)</sup>].

as another possible reason for the superior properties of  $\text{Co}_5\text{Sm}$ . Domain measurements were also used to estimate  $D_c$  for various 17-2 and 7-2 compounds, and it was found that only  $\text{Co}_5\text{Gd}$  and  $\text{Co}_7\text{Gd}_2$  had larger  $D_c$  values than  $\text{Co}_5\text{Sm}$ .<sup>(57, 58)</sup> In both of these compounds, high coercivities are easily attained in ground powders.<sup>(59)</sup>

### Sintered Magnets

Domain studies on sintered  $\text{Co}_5\text{Sm}$  magnets<sup>(60)</sup> show that each grain contains several domains in the thermally demagnetized condition, and that these domains move about easily throughout most of the material. Hence, general wall pinning remains low. Once the magnet is magnetized, however, most grains apparently reverse abruptly in a "single-domain" process, and only a minority of grains show an internal domain structure. Individual grains can resist reversal to high fields despite the early reversal of neighboring grains, indicating either strong pinning at the grain boundary or no exchange contact between grains.

The coercivity of sintered  $\text{Co}_5\text{Sm}$ -based magnets depends sensitively on composition, sintering temperature and time, and post-sintering heat treatment (Refs. 1, 25, 61-66). Maximum coercivity occurs when the  $\text{Co}_5\text{Sm}$  phase reaches the Sm-rich limit of its composition range.<sup>(67, 68)</sup> (Total Sm content would be well into the two-phase range, but account is taken of the Sm tied up in the form of  $\text{Sm}_2\text{O}_3$ .) It is not yet clear how much of this composition sensitivity is caused by a dependence of  $K$  on deviations from stoichiometry, and how much is caused by a change in defect distribution. Benz and Martin<sup>(67)</sup> have suggested that cobalt vacancies present in hyperstoichiometric alloys not only accelerate sintering, but also aid coercivity. The deleterious effect of heat treatments near  $700^\circ\text{C}$  is probably caused by eutectoid decomposition, as mentioned above. The beneficial effect of heat treatment near  $900^\circ\text{C}$  may result from the dissolution of cobalt-rich regions associated with residual composition inhomogeneities<sup>(69)</sup> or formed by eutectoid decomposition during prior cooling.

Several investigators have produced good properties in sintered magnets by blending together powders of two different compositions, one of which is rare-earth-rich and liquid at the sintering temperature.<sup>(1, 70)</sup> This and other observations led Schweizer *et al.*<sup>(71)</sup> to suggest a modification of Zijlstra's surface-pinning theory in which each  $\text{Co}_5\text{Sm}$  grain is presumed enclosed by an epitaxial  $\text{Co}_2\text{Sm}_2$  shell, which contains pinning sites. However, there has been no direct evidence of the existence of such a shell, and experience indicates that high coercivities can also be obtained without the use of a liquid-phase sintering additive.

Martin and Benz<sup>(72)</sup> recently measured the temperature dependence of coercivity in a number of sintered magnets of varying coercivity, and found that the results could all be normalized to a single curve

representing the increase of relative coercivity with decreasing temperature (Fig. 7). They also measured the temperature dependence of the anisotropy constant  $K$  for one of these magnets, and found it identical to the temperature dependence of coercivity (Fig. 8).<sup>(73)</sup> This suggests that thermal activation plays no major role in producing the temperature dependence of coercivity. This is in contrast to the view of other workers<sup>(52, 74, 75)</sup> who had noted that coercivity was much more temperature-dependent than the anisotropy

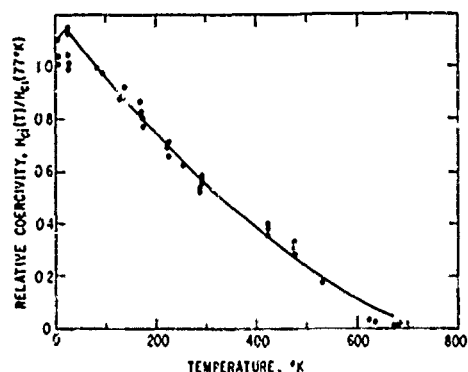


Fig. 7 Relative coercivity vs temperature for a series of  $\text{Co}_5\text{Sm}$  sintered magnets [from Martin and Benz<sup>(72)</sup>].

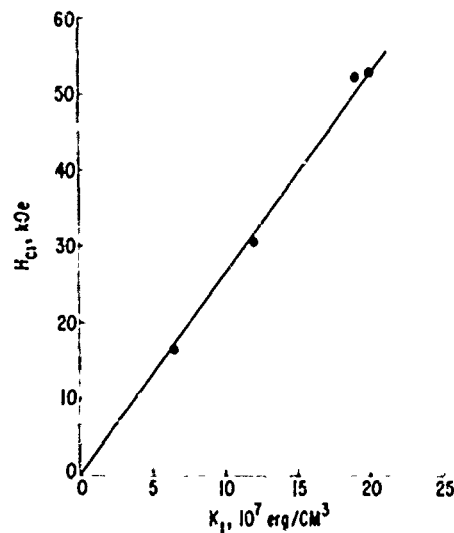


Fig. 8 Coercivity vs anisotropy constant (measured at various temperatures) for a  $\text{Co}_5\text{Sm}$  sintered magnet [from Benz and Martin<sup>(73)</sup>].

constants reported by Tatsumoto *et al.*<sup>(6)</sup> However since the anisotropy measurements of Benz and Martin were obtained with much larger measuring fields, they are probably more reliable. Because of the likely variation of  $K$  with deviations from stoichiometry, it is also highly desirable to measure coercivity and  $K$  on the same samples, as did Benz and Martin. Nesbitt *et al.*<sup>(29)</sup> measured coercivity and  $K$  on a single crystal of a Co-Fe-Cu-Cr alloy, in which



coercivity is controlled by general wall pinning. Most of the temperature dependence of coercivity could be explained by the temperature dependence of  $k$  in this case as well.

Domain studies of sintered magnets water-quenched from high temperatures have shown the existence of a surface layer of low-coercivity grains about 200 $\mu$  thick.<sup>(76)</sup> This layer accounts for the kinked magnetization curves previously reported.<sup>(77)</sup> Further studies indicate that this layer is caused by thermal stresses produced from the temperature gradients during quenching.<sup>(76)</sup>

#### CONCLUSIONS

Since coercivities so far obtained are far below 2K/M<sub>S</sub>, it is clear that coherent rotation or incoherent rotation processes such as curling do not operate. Except in the copper-bearing precipitation alloys, general wall pinning is low. Domain nucleation and local wall pinning both influence coercivity, and are even interrelated in some models. However, since most experiments suggest that defects decrease coercivity, coercivity appears to be limited primarily by domain nucleation.

The specific defects responsible for nucleation, or for local pinning, have not been conclusively identified. The effects of low-temperature aging of powders, and of composition and heat treatment on sintered magnets, suggest that low-K cobalt rich regions may serve as defects for domain nucleation. The effects of grinding on powders and of thermal stresses on sintered magnets suggest that plastic deformation may produce nucleation sites, presumably either dislocations or stacking faults.

The superiority of Co<sub>5</sub>Sm to other cobalt-rare earth compounds is attributable in part to the higher  $K$ , which results in a higher  $\gamma$  and a higher  $D_c$ . Another possible factor is less sensitivity of  $K$  to composition, particularly increases in cobalt concentration. (This can be inferred from the observation that Co<sub>17</sub>Sm<sub>3</sub> remains easy-axis while most of the other Co<sub>17</sub>R<sub>3</sub> compounds are easy-plane, i. e., they have negative  $K$ .)<sup>(3)</sup>

More information is needed on the dependence of  $K$  on deviations from stoichiometry. Measurements of magnetostriction coefficients are necessary to assess the importance of dislocations. [Some data already exist for Co-Gd compounds.<sup>(78)</sup>] Experimental and theoretical study of various stacking faults possible in these systems would help assess their importance. More metallurgical work focused on the grain boundaries in sintered magnets would help us understand how neighboring grains remain so magnetically independent.

#### ACKNOWLEDGMENTS

I am grateful to J. J. Becker for many interesting and educational discussions and for a critical reading of the manuscript. M. G. Benz and D. L. Martin pro-

vided helpful discussions about sintered magnets. This work was supported by the Advanced Research Projects Agency, Department of Defense, and was

monitored by the Air Force Materials Laboratory, MAFEL, under Contract F33615-70-C-1626.

#### REFERENCES

1. D. L. Martin and M. G. Benz, Proc. 1971 Conf. on Magnetism and Magnetic Materials, A. I. P. Conf. Proc. 5, 970 (1970).
2. K. J. Straat, ibid., p. 1047.
3. J. J. Becker, J. Appl. Phys. 41, 1055 (1970).
4. G. Hoffer and K. Straat, IEEE Trans. Mag. 2, 487 (1966).
5. K. H. Buschow and W. A. J. J. Veige, Z. angew. Phys. 26, 157 (1969).
6. E. Tatsumoto, J. Okamoto, H. Fujii, and C. Inoue, Suppl. J. Physique 32, C1-550 (1971).
7. K. Straat, G. Hoffer, J. Olson, W. Ostertag, and J. J. Becker, J. Appl. Phys. 38, 1001 (1967).
8. D. J. Craik and R. S. Tebble, Ferromagnetism and Ferromagnetic Domains, John Wiley and Sons, Inc., New York (1965), p. 47.
9. C. Kooy and U. Enz, Philips Res. Repts. 15, 7 (1960).
10. W. F. Brown, Jr., Micromagnetics, Interscience, New York (1963).
11. E. C. Stoner and E. P. Wohlfarth, Phil. Trans. Roy. Soc. London A240 599 (1948).
12. K. H. J. Buschow, P. A. Naastepad, and F. F. Westendorp, IEEE Trans. Mag. 9, 301 (1970).
13. S. Shtrikman and D. Treves, J. Appl. Phys. Suppl. 31, 72S (1960).
14. U. Dehlinger and A. Holz, Z. Metallk. 59, 822 (1968); A. Holz, Phys. Stat. Sol. 25, 567 (1968); J. Appl. Phys. 41, 1095 (1970).
15. H. Zijlstra, Z. angew. Phys. 21, 6 (1966); IEEE Trans. Mag. 6, 179 (1970).
16. R. Carey and B. W. J. Thomas, J. Phys. D: Appl. Phys. 5, 200 (1972).
17. A. Aharoni, Rev. Mod. Phys. 34, 227 (1962); Phys. Stat. Sol. 16, 3 (1966).
18. C. Abraham and A. Aharoni, Phys. Rev. 128, 2496 (1962).

19. H. Zijlstra and H. B. Haanstra, *J. Appl. Phys.* 37, 2853 (1966).
20. K. Becker and W. Döring, *Ferromagnetismus*, Springer, Berlin (1939), p. 192.
21. L. J. Dijkstra, in *Thermodynamics in Physical Metallurgy*, American Society for Metals, Cleveland (1950), p. 271.
22. R. Carey, J. F. Coleman, and I. V. F. Viney, *Proc. Roy. Soc. London* A328, 143 (1972).
23. H. Zijlstra, *J. Appl. Phys.* 41, 4881 (1970).
24. P. Haasen, *Mater. Sci. Eng.* 9, 191 (1972).
25. F. F. Westendorp, *Sol. State Commun.* 8, 139 (1970).
26. H. Zijlstra, *J. Appl. Phys.* 42, 1510 (1971).
27. J. J. van den Broek and H. Zijlstra, *IEEE Trans. Mag.* 7, 226 (1970).
28. D. J. Craik, *Proc. Internat. Conf. on Magnetism*, Nottingham, Inst. of Physics and Physical Soc., London (1964), p. 693.
29. E. A. Nesbitt, G. Y. Chin, G. W. Hull, R. C. Sherwood, M. L. Green and J. H. Wernick, *Proc. 1972 Conf. on Magnetism and Magnetic Materials*, A. I. P. Conf. Proc. 10, (1973).
30. J. J. Becker, *IEEE Trans. Mag.* 4, 239 (1968).
31. J. J. Becker, *J. Appl. Phys.* 39, 1270 (1968).
32. D. J. Craik and D. A. McIntyre, *Phys. Letters* 21, 288 (1966).
33. M. Rosenberg, C. Tanasoiu, and V. Florescu, *Phys. Letters* 23, 540 (1966).
34. Ya. S. Shur and V. I. Khrabrov, *Sov. Phys. -JETP* 30, 1027 (1970).
35. Ya. S. Shur, E. V. Shtol'ts, and V. L. Margolina, *Sov. Phys. -JETP* 11, 33 (1960).
36. Ya. S. Shur, A. V. Deryagin, T. V. Sysolina, and G. S. Kandaurova, *Phys. Met. Metallog.* 30, 12 (1970).
37. J. J. Becker, *J. Appl. Phys.* 42, 1537 (1971).
38. J. J. Becker, *IEEE Trans. Mag.* 7, 644 (1971).
39. J. J. Becker, *IEEE Trans. Mag.* 5, 211 (1969).
40. R. C. Sherwood, J. P. Remelka, and H. J. Williams, *J. Appl. Phys.* 30, 217 (1959).
41. J. J. Becker, *IEEE Trans. Mag.* 8 (1972).
42. S. Reich, S. Shtrikman, and D. Treves, *J. Appl. Phys.* 36, 140 (1965).
43. J. J. Becker, *Proc. 1971 Conf. on Magnetism and Magnetic Materials*, A. I. P. Conf. Proc. 5, 1067 (1972).
44. K. J. Strnat, J. C. Olson, and G. Hoffer, *Proc. 6th Rare Earth Res. Conf.*, Gatlinburg, Tenn., 603 (1967).
45. K. J. Strnat, J. C. Olson, and G. Hoffer, *J. Appl. Phys.* 39, 1263 (1968).
46. R. A. McCurrie, G. I. Carswell, and J. B. O'Neill, *J. Mater. Sci.* 5, 164 (1970).
47. R. A. McCurrie and G. P. Carswell, *J. Mater. Sci.* 5, 825 (1970).
48. K. H. J. Buschow, P. A. Naastepad, and F. F. Westendorp, *J. Appl. Phys.* 40, 4029 (1969).
49. F. F. Westendorp, *IEEE Trans. Mag.* 6, 472 (1970).
50. J. J. Becker and R. E. Cech, U.S. Patent No. 3,615,914, filed 1968, patented 1971.
51. J. J. Becker, *J. Appl. Phys.* 38, 1015 (1967).
52. R. A. McCurrie, *Phil. Mag.* 22, 1013 (1970).
53. R. A. McCurrie and G. P. Carswell, *Phil. Mag.* 2, 333 (1971).
54. F. A. J. den Broeder and K. H. J. Buschow, *J. Less-Common Metals* 29, 65 (1972).
55. K. H. J. Buschow, *ibid.*, p. 283.
56. F. F. Westendorp, *J. Appl. Phys.* 42, 5727 (1971).
57. J. D. Livingston, *J. Appl. Phys.*, 43, 4756 (1972).
58. J. D. Livingston, *J. Mater. Sci.*, to be published.
59. K. H. J. Buschow and A. S. van der Goot, *J. Less-Common Metals* 17, 249 (1969).
60. J. D. Livingston, unpublished research.
61. D. L. Martin and M. G. Benz, *Cobalt* 50, 11 (1971).
62. M. G. Benz and D. L. Martin, *J. Appl. Phys.* 42, 2786 (1971).
63. M. G. Benz and D. L. Martin, *Proc. 1971 Conf. on Magnetism and Magnetic Materials*, A. I. P. Conf. Proc. 5, 1082 (1972).

64. R. J. Charles, D. L. Martin, L. Valentine, and R. E. Cech, ibid., p. 1072.
65. R. E. Cech, J. Appl. Phys. 41, 5247 (1970).
66. D. K. Das, IEEE Trans. Mag. 7, 432 (1971).
67. M. G. Benz and D. L. Martin, J. Appl. Phys. 43, 2165 (1972).
68. M. G. Benz, D. L. Martin, and A. C. Rockwood, Proc. 1972 Conf. on Magnetism and Magnetic Materials, A. I. P. Conf. Proc. 10, (1973).
69. A. Menth, Proc. 1972 Conf. on Magnetism and Magnetic Materials, A. I. P. Conf. Proc. 10, (1973).
70. M. G. Benz and D. L. Martin, Appl. Phys. Letters 17, 176 (1970).
71. J. Schweizer, K. J. Strnat, and J. B. Y. Tsui, IEEE Trans. Mag. 7, 429 (1971).
72. D. L. Martin and M. G. Benz, IEEE Trans. Mag. 8, (1972).
73. M. G. Benz and D. L. Martin, J. Appl. Phys., to be published.
74. R. A. McCurrie, Proc. 1972 Conf. on Magnetism and Magnetic Materials, A. I. P. Conf. Proc. 10, (1973).
75. P. Gaunt, J. Appl. Phys. 43, 637 (1972).
76. F. G. Jones, J. D. Livingston, and J. G. Smeggil, unpublished research.
77. F. G. Jones, H. E. Lehman, and J. G. Smeggil, IEEE Trans. Mag. 8, (1972).
78. O. A. W. Strydom and I. Alberts, J. Less-Common Metals 22, 503 (1970).
79. A. E. Ray, H. Mildrum, K. Strnat, and R. Harner, Suppl. J. de Physique 32, C1-554 (1971).
80. H. Mildrum, A. E. Ray, and K. Strnat. Proc. 8th Rare Earth Res. Conf. Vol. 1, 21 (1970).
81. K. Strnat, Cobalt 36, 133 (1967).
82. K. Strnat, A. E. Ray, and C. Herget, Suppl. J. de Physique 32, C1-552 (1971).
83. K. Strnat and J. Tsui, Proc. 8th Rare Earth Res. Conf., Vol. 1, 3 (1970).

### III. MATERIALS CHARACTERIZATION AND PHASE EQUILIBRIUM STUDIES

#### 1. Studies of the decomposition of $\text{Co}_5\text{Sm}$ at elevated temperatures (J. G. Smeggil)

---

Cast Co-Sm alloys were prepared having overall compositions such that they consisted of two phases, either  $\text{Co}_5\text{Sm} + \text{Co}_7\text{Sm}_2$  or  $\text{Co}_5\text{Sm} + \text{Co}_{17}\text{Sm}_2$ . These alloys were annealed at  $750^\circ\text{C}$  for periods up to several weeks. The samples were protected from oxidation by wrapping in Zr and Mo foils, and heated in an argon atmosphere.

Subsequent examination of these samples is being carried out using x-ray techniques, analytical chemistry, electron microprobe analysis, scanning electron microscopy, and optical metallography. At present this work is still in progress.

Figures 1 and 2 represent a sample of  $\text{Co}_5\text{Sm} + \text{Co}_7\text{Sm}_2$  as cast and as annealed for 21 days. Electron microprobe work indicates that the background phase is  $\text{Co}_7\text{Sm}_2$  while the lighter patches are  $\text{Co}_5\text{Sm}$ . The striations in the  $\text{Co}_5\text{Sm}$  regions of the sample annealed 21 days are only observable after etching. Scanning electron microscopy of this sample shows that the lines are etched-out lamelle.

Similar studies of a material containing  $\text{Co}_5\text{Sm} + \text{Co}_{17}\text{Sm}_2$  again show a striated structure developing in the  $\text{Co}_5\text{Sm}$  phase after extended periods of annealing.

Two-phase alloys were used in order that the  $\text{Co}_5\text{Sm}$  phase could be studied at both ends of the homogeneity range present when it is formed. Further studies are under way in single-phase alloys of these compositions. The objective is to see whether the decomposition takes place as a simple precipitation reaction, or, as suggested by Bushow, eutectoidally. Our preliminary results suggest the former, rather than the appearance of two new phases from the decomposing phase required by Buschow's model.

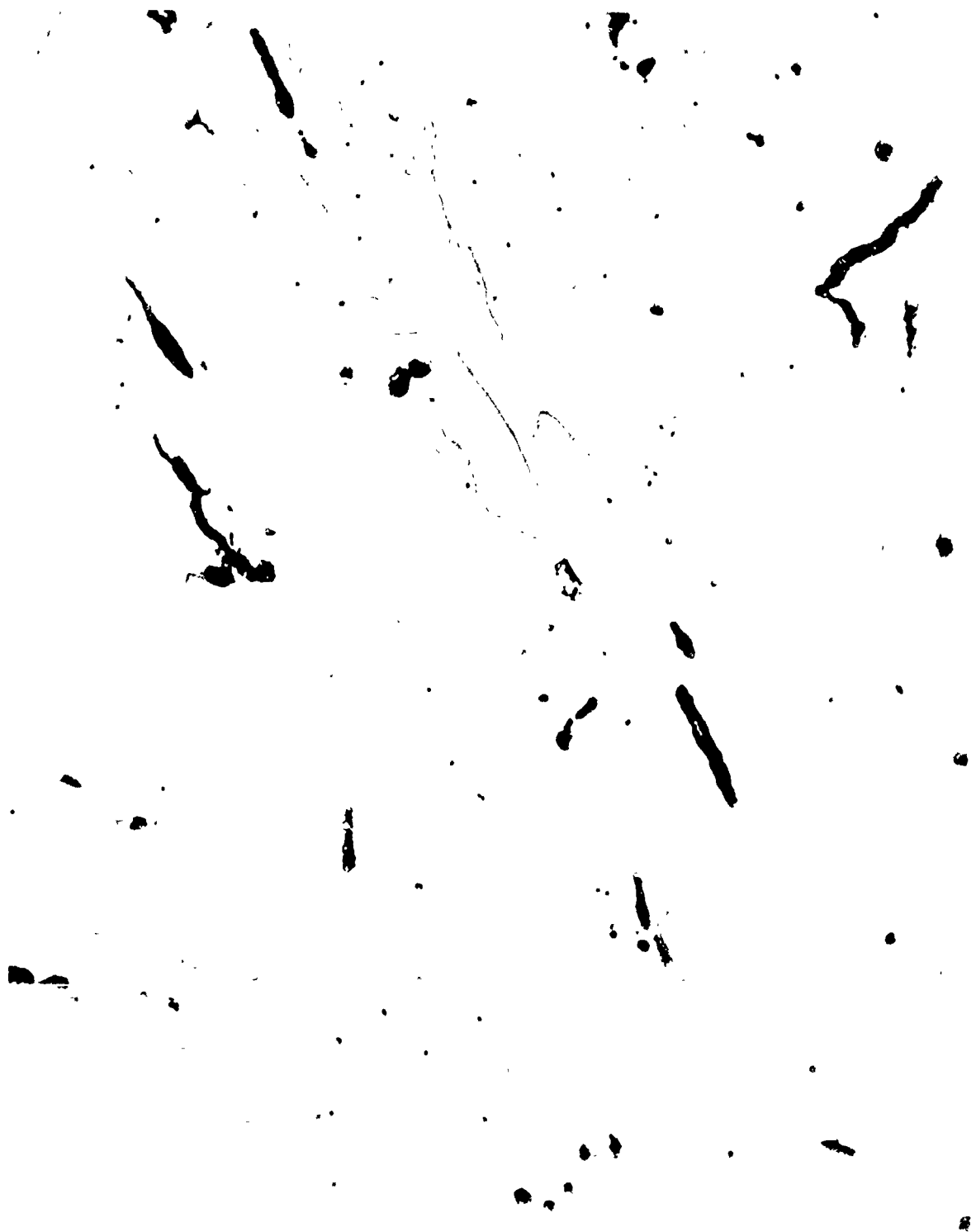


Figure 1  $\text{Co}_5\text{Sm} + \text{Co}_7\text{Sm}_2$ . As cast. Etched with 1% nital - 5% hydrol. 1000X



Figure 2  $\text{Co}_5\text{Sm} + \text{Co}_7\text{Sm}_2$ . Annealed 21 days at  $750^\circ\text{C}$ . Etched with 1% nital - 5% hydrol. 1000X

#### IV. ALLOY STUDIES

##### 1. Preparation and examination of Co<sub>5</sub>Tm, Co<sub>5</sub>Yb, Co<sub>5</sub>Sc, Co<sub>5</sub>Eu, and Co<sub>5</sub>Lu (J. D. Livingston)

Attempts were made to cast alloys of nominal compositions corresponding to Co<sub>5</sub>Tm, Co<sub>5</sub>Yb, Co<sub>5</sub>Sc, Co<sub>5</sub>Eu, and Co<sub>5</sub>Lu. The Co-Tm casting exhibited a lamellar microstructure (Fig. 1) which showed an intricate pattern of magnetic domains when viewed under polarized light (Fig. 2). X-ray powder patterns indicate the presence of Co<sub>5</sub>Tm and Co<sub>7</sub>Tm<sub>2</sub>. The Co-Yb and Co-Sc castings consisted of Co-rich dendrites and an interdendritic eutectic (Figs. 3 and 4). X-ray powder patterns indicate Co, Co<sub>17</sub>Yb<sub>2</sub>, and possibly Co<sub>5</sub>Yb in the former casting and Co<sub>2</sub>Sc in the latter. The Co-Eu casting was very inhomogeneous and a portion was very reactive. No intermetallic compounds were detected, but Eu(OH)<sub>3</sub> was prominent in the x-ray patterns. The Co-Lu melt reacted violently and rapidly with the alumina crucible, and no casting could be prepared.

##### 2. Variation of mechanical hardness and coercive force with post-sintering heat treatment (J. G. Smeggil)

Hardness measurements were made on cylindrical liquid-phase-sintered Co<sub>5</sub>Sm magnets using a Knoop indenter. The samples were sintered at 1100°C for 1/2 hour, then annealed at either 750°, 900°, or 1100°C for 1/2 hour. A circular cross-section was polished on each specimen. A 200-gram load was applied to the indenter at a rate of 0.05 mm/sec for 10 seconds. The hardness values and coercive forces observed on these samples are as follows:

<u>T(°C)</u>	<u>KHN (kg/mm<sup>2</sup>)</u>	<u>H<sub>ci</sub>(kOe)</u>
750	541 (±54)	1.2
900	575 (±40)	20.3
1100	618 (±51)	2.0

The hardness data are in agreement with those reported in McCurrie, Carswell, and O'Neill, J. Mater. Sci. 6, 164 (1970). Even though the hardness values are the same within experimental error, the coercive forces vary by a factor of twenty.

##### 3. Diffusion studies (D. L. Martin)

Diffusion couples have been made between cobalt and a 60 wt% Sm alloy. The diffusion zone clearly shows layers of 17-2, 5-1, 7-2, and 3-1 compounds.

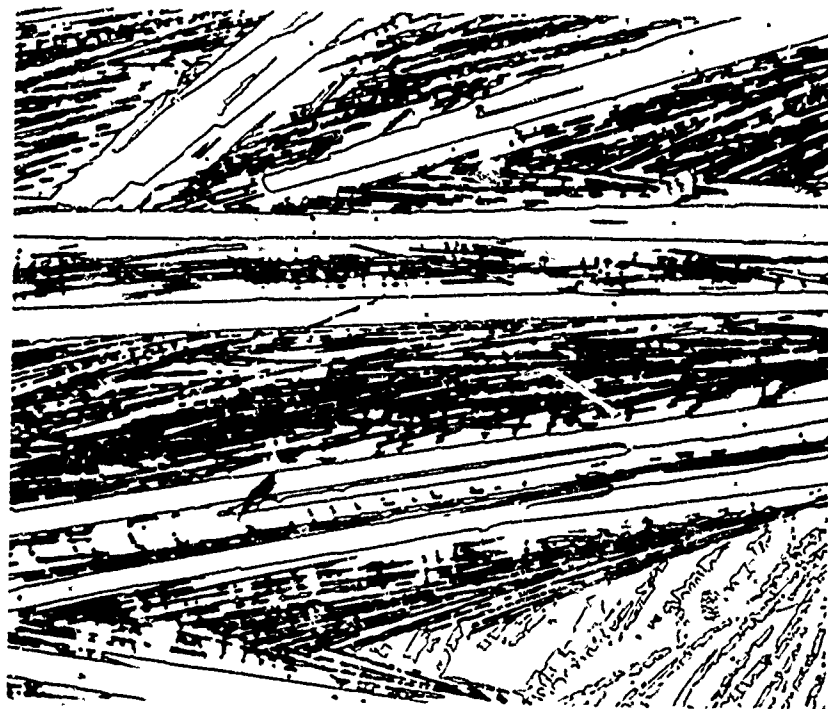


Figure 1 Co-Tm as-cast.

174X



Figure 2 Co-Tm as-cast (domains).

174X



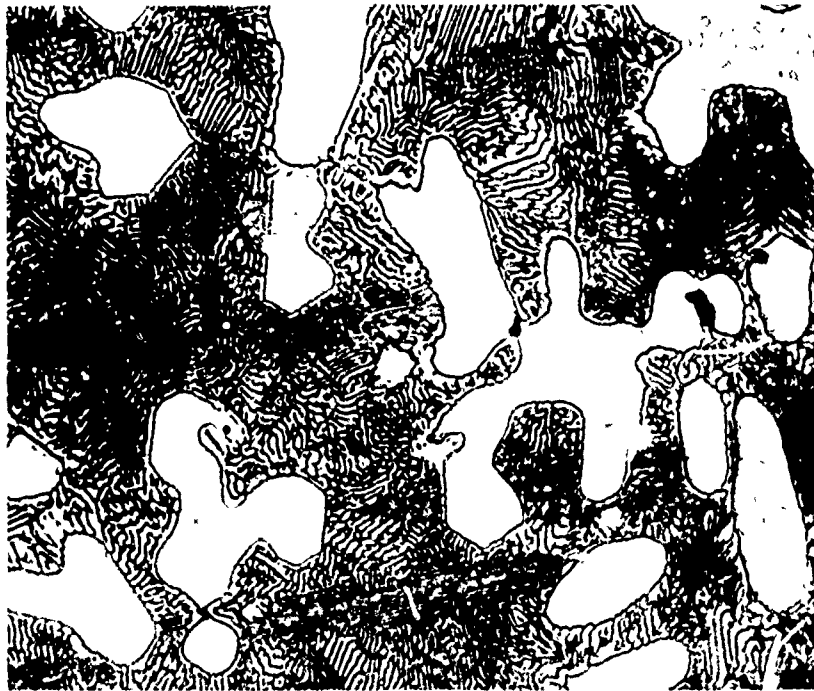


Figure 3 Co-Sc as-cast.

560X



Figure 4 Co-Yb as-cast.

336X

Magnetic domain observations indicate that the 5-1 phase is oriented with its c-axis along the diffusion direction. These studies are designed to elucidate the reactions occurring in the sintering process and to aid in the positive identification of phases observed by optical metallography in cast alloys and sintered magnets. Preliminary results are definitely encouraging and indicate that this technique will be a valuable tool.

4. COBALT-SAMARIUM PERMANENT MAGNET ALLOYS:  
VARIATION OF LATTICE PARAMETERS WITH  
COMPOSITION AND TEMPERATURE

D. L. Martin, M. G. Benz, and A. C. Rockwood

(To be published in AIP Conference Proceedings)

**GENERAL  ELECTRIC**

**GENERAL ELECTRIC COMPANY  
CORPORATE RESEARCH AND DEVELOPMENT**

**Schenectady, N.Y.**

---

---

---

---

---

---

**COBALT-SAMARIUM PERMANENT MAGNET ALLOYS:  
VARIATION OF LATTICE PARAMETERS  
WITH COMPOSITION AND TEMPERATURE**

by

**D. L. Martin, M. G. Benz, and A. C. Rockwood  
Metallurgy and Ceramics Laboratory**

**Report No. 72CRD310**

**November 1972**

---

---

---

---

---

---

**TECHNICAL INFORMATION SERIES**

**CLASS 1**

41

General Electric Company  
Corporate Research and Development  
Schenectady, New York

<small>AUTHOR</small> Martin, DL Benz, MG Rockwood, AC	<small>SUBJECT</small> permanent magnets	<small>NO</small> 72CRD310
		<small>DATE</small> November 1972
<small>TITLE</small> Cobalt-Samarium Permanent Magnet Alloys: Variation of Lattice Parameters with Composition and Temperature		<small>GE CLASS</small> 1
		<small>NO. PAGES</small> 4
<small>ORIGINATING COMPONENT</small> Metallurgy and Ceramics Laboratory		<small>CORPORATE RESEARCH AND DEVELOPMENT SCHENECTADY, N.Y.</small>
<small>SUMMARY</small> <p>Previous studies have shown that the magnetic properties of <math>\text{Co}_5\text{Sm}</math> permanent magnets are greatly improved when the composition after sintering is hyperstoichiometric (Sm rich).</p> <p>In this study, x-ray lattice parameters, chemical composition, phase identification by metallography and magnetic properties have been measured for a series of closely spaced composition, in order to determine conclusively the phases present at the optimum composition. From these observations, one can conclude that the peak magnetic properties do indeed occur when the composition is hyperstoichiometric; i. e., close to the <math>\text{Co}_5\text{Sm}-\text{Co}_7\text{Sm}_2</math> phase boundary as determined by x-ray measurements, 16.85 at. % Sm as determined by measurements of the chemical composition.</p> <p>In addition, changes in lattice parameter with temperature over the range <math>77^\circ</math> to <math>300^\circ\text{K}</math> are reported.</p>		
<small>KEY WORDS</small> permanent magnets, cobalt-samarium, lattice parameters		

INFORMATION PREPARED FOR \_\_\_\_\_

Additional Hard Copies Available From

Corporate Research & Development Distribution  
P.O. Box 43 Bldg. 5, Schenectady, N.Y., 12301

Microfiche Copies Available From

Technical Information Exchange  
P.O. Box 43 Bldg. 5, Schenectady, N.Y., 12301

COBALT-SAMARIUM PERMANENT MAGNET ALLOYS:  
VARIATION OF LATTICE PARAMETERS WITH COMPOSITION AND TEMPERATURE

P. L. Martin, M. G. Benz, and A. C. Rockwood

INTRODUCTION

The peak magnetic properties for  $\text{Co}_5\text{Sm}$ -type magnets are obtained in alloys with samarium in excess of the stoichiometric composition, that is, about 37 wt% Sm vs 33.8 wt% Sm in  $\text{Co}_5\text{Sm}$ .<sup>(1-3)</sup> The samarium in the magnet sample may be present as cobalt-samarium alloy phases or as samarium oxide. Oxygen is unavoidable in these alloys because of the high reactivity of powders containing samarium. A sintered magnet might contain as much as 0.4 wt% oxygen. This amount of oxygen would combine with 2.5 wt% Sm to form 2.9 wt%  $\text{Sm}_2\text{O}_3$ . Therefore, it is important to adjust for  $\text{Sm}_2\text{O}_3$  in determining the amount of samarium available to combine with the cobalt.

In a recent study,<sup>(4)</sup> we showed that the peak intrinsic coercive force,  $H_{ci}$ , occurred at an adjusted composition of 17.3 at. % samarium compared to 16.7 at. % samarium for stoichiometric  $\text{Co}_5\text{Sm}$ . A correlation was observed also between sintering shrinkage and coercive force. The alloys showing the greatest shrinkage also possessed the highest coercive force. A model for the mechanism of sintering was postulated where the slow step was the diffusion of samarium atoms in the grain-boundary regions via a samarium-atom-cobalt-vacancy cluster exchange mechanism. Central to the considerations advanced for the sintering model are the point defect structures which lead to a broad  $\text{Co}_5\text{Sm}$ , homogeneity region extending beyond the stoichiometric composition to higher samarium alloys. Such a region has been reported to exist above 800°C and, at 1200°C to extend from 14.5 at. % Sm to the hyperstoichiometric composition of 17.0 at. % Sm.<sup>(5)</sup>

EXPERIMENTAL

The samples were prepared by careful blending of two powders using different ratios to vary the composition. The chemical compositions (wt %) of the base metal and additive powder were as follows:

	Co	Sm	$\text{O}_2$	Ni	Al
Base	65.4	33.9	0.24	0.05	0.05
Additive	39.4	59.6	0.76	0.19	< 0.01

These powders were blended into 12 closely spaced mixes covering the range 16.25 to 17.5 at. % Sm after adjusting for  $\text{Sm}_2\text{O}_3$ . The blended powders were aligned, pressed, and sintered for 1 hour 1120°C in argon. The samples were cooled slowly from the sintering temperature to 900°C, and then rapidly in a cooling chamber. The chemical composition of Sample F was determined by analytical means as a check on the calculated compositions. Its composition was found to be: 64.0 wt% Co, 35.2% Sm, 0.05% Ni, 0.05% Al, and 0.33%  $\text{O}_2$ . This corresponds to an adjusted alloy

composition of 16.85 at. % Sm as compared to the value of 16.84 at. % Sm calculated from the analyses for the base metal and additive powders. This agreement is better than is to be expected in view of an experimental error of  $\pm 0.2$  wt% for Co and Sm analysis; nevertheless, it does give credence to the accuracy of the blending procedure.

RESULTS AND DISCUSSION

X-ray Parameter Data.

The lattice parameters were determined from the powder diffraction x-ray data ( $\text{Co-K}\alpha$  and  $\text{Fe-K}\alpha$  radiation) by well-known methods.<sup>(6,7)</sup> The  $a_0$  and  $c_0$  results are plotted in Fig. 1 together with the density

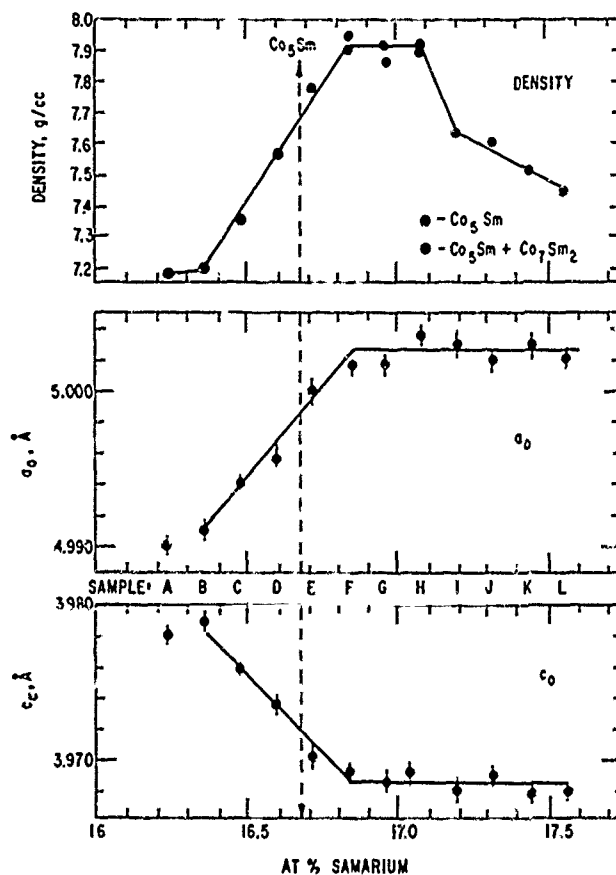


Fig. 1 Change of  $\text{Co}_5\text{Sm}$  lattice parameters and density with adjusted samarium content.

The x-ray parameter values for  $\text{Co}_5\text{Sm}$  become constant for alloys containing more than 16.85 at. % Sm. The constant level of the x-ray parameters signifies a two-phase field, and the inflection point indicates the end of the  $\text{Co}_5\text{Sm}$  phase field and the beginning of the  $\text{Co}_5\text{Sm} + \text{Co}_7\text{Sm}_2$  two-phase field. X-ray

diffraction methods are generally insensitive to small volume fractions of a second phase so that the presence of the  $\text{Co}_7\text{Sm}_2$  phase was detected first by x-ray means in Sample I (17.2 at. % Sm). Microscopic examination is a more sensitive method and it showed small, isolated  $\text{Co}_7\text{Sm}_2$  particles in Sample E (16.72 at. % Sm).

The change in the  $a_0$  and  $c_0$  lattice parameters with composition below 16.8 at. % Sm is evidence for the existence of a broad homogeneity range as already reported.<sup>(5, 8)</sup> While our results indicate that this homogeneity range extends slightly beyond the  $\text{Co}_6\text{Sm}$  stoichiometric composition to higher samarium alloys, the chemical analysis error is such that it is difficult to determine the absolute position of the stoichiometric composition.

The lattice parameter data are in good agreement with those published by others if one takes into consideration the measurement error. In Table I, published x-ray data for  $\text{Co}_6\text{Sm}$  samples located near the  $\text{Co}_6\text{Sm}$ - $\text{Co}_7\text{Sm}_2$  boundary are compared with our data.

#### Density and Metallographic Results

Note in Fig. 1 that the density peaks near the  $\text{Co}_6\text{Sm}$ - $\text{Co}_7\text{Sm}_2$  boundary and falls rapidly a short distance on either side of the boundary.

The  $\text{Co}_7\text{Sm}_2$  phase was detected by metallographic examination in Samples E to L. This would place the  $\text{Co}_6\text{Sm}$ - $\text{Co}_7\text{Sm}_2$  boundary at about 17.7 at. % Sm compared to a value of 17.85 at. % Sm as indicated by the break in the  $a_0$  or  $c_0$  curves.

#### Magnetic Measurements

The change of magnetic properties with composition is shown in Fig. 2. A summary of pertinent magnetic data and other information is listed in Table II. The highest values of coercive force and  $(BH)_{\text{max}}$  are obtained in the same region where the

density peaks, and the lattice parameter values become constant. The magnetic properties, in particular the  $H_{ci}$  and  $H_c$  values, drop rapidly on either side of the boundary, although the drop is more severe on the cobalt-rich side than on the samarium-rich side. However, it should be noted that Samples C and D (16.48 and 16.60 at. % Sm), which do not

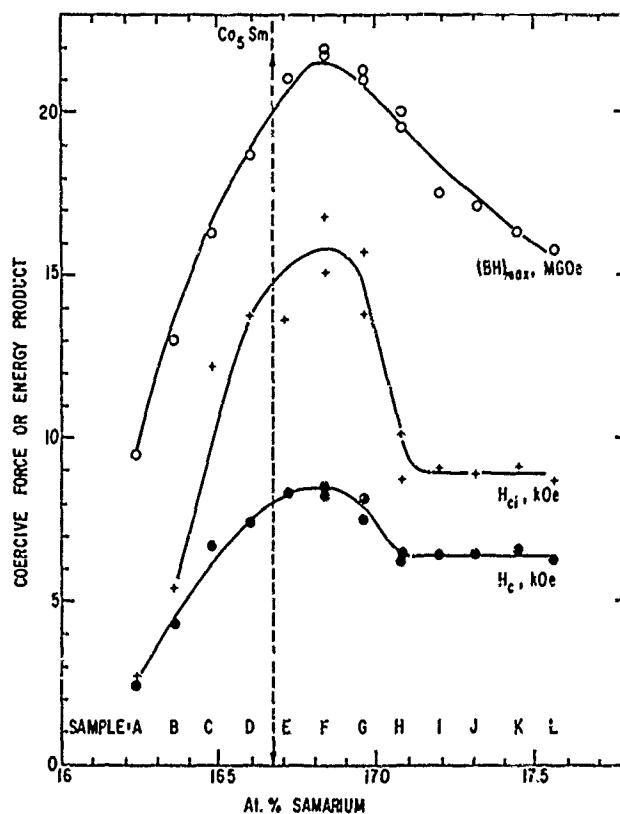


Fig. 2 Magnetic properties after sintering and aging as a function of the adjusted samarium content of the Co-Sm alloy phase or phases.

TABLE I  
X-ray Data for  $\text{Co}_6\text{Sm}$  Near the  $\text{Co}_6\text{Sm}$ - $\text{Co}_7\text{Sm}_2$  Boundary

Reference	Exptl Error ( $\text{\AA}$ )	a ( $\text{\AA}$ )	c ( $\text{\AA}$ )	c/a	Vol. ( $\text{\AA}^3$ )
Umehayashi and Fujimura <sup>(8)</sup>	$\pm 0.002$	5.004	3.969	0.793	86.17
Austin and Miller <sup>(9)</sup>	$\pm 0.002$	5.002	3.969	0.793	86.10
Buschow and Van der Goot <sup>(5)</sup>	$\pm 0.005$	4.995	3.965	0.794	85.74
Velge and Buschow <sup>(10)</sup>	$\pm 0.005$	5.004	3.969	0.793	86.14
Haszko <sup>(11)</sup>	$\pm 0.005$	5.004	3.971	0.794	86.18
This study--Sample E	$\pm 0.001$	5.000	3.972	0.794	86.08
This study--Sample F	$\pm 0.001$	5.0015	3.9692	0.794	86.08
This study--Sample G	$\pm 0.001$	5.0017	3.9686	0.793	86.08
Average		5.002	3.969	0.793	86.07

Table II  
Summary of Data for a Co-Sm Alloy Series

Sample	At. % Sm*	Co <sub>7</sub> Sm <sub>2</sub>	4π J <sub>S</sub> (kG)	B <sub>r</sub> (kG)	H <sub>c</sub> (kOe)	jH <sub>c</sub> kOe	(BH) <sub>max</sub> (MCOe)	Density (g/cc)
A	16.24	No	10.4	8.4	2.4	2.7	9.5	7.18
B	16.36	No	10.4	8.6	4.3	5.4	13.0	7.20
C	16.48	No	10.3	8.7	6.7	12.2	16.3	7.36
D	16.60	No	10.4	9.0	7.4	13.7	18.7	7.57
E	16.72	Yes	10.4	9.3	8.3	13.6	21.0	7.78
F	16.84	Yes	10.4	9.5	8.5	16.8	21.9	7.94
F-2	16.84	Yes	10.4	9.4	8.2	15.1	21.8	7.91
G	16.96	Yes	10.3	9.3	8.1	15.7	21.3	7.92
G-2	16.96	Yes	10.3	9.3	7.5	13.8	21.0	7.87
H	17.08	Yes	10.1	9.1	6.5	10.1	19.5	7.90
H-2	17.08	Yes	10.3	9.2	6.2	8.7	20.0	7.93
I	17.20	Yes †	9.9	8.6	6.4	9.1	17.5	7.64
J	17.32	Yes †	9.8	8.5	6.4	8.9	17.1	7.61
K	17.45	Yes †	9.6	8.3	6.6	9.1	16.3	7.53
L	17.56	Yes †	9.6	8.2	6.3	9.7	15.8	7.45

\* Calculated on assumption that oxygen forms Sm<sub>2</sub>O<sub>3</sub>.

† Detected by x-ray as well as by metallographic examination.

contain Co<sub>7</sub>Sm<sub>2</sub>, have relatively high values of coercive force. Beyond 17.1 at. % Sm, the coercive force (H<sub>c1</sub> and H<sub>c</sub>) level out with increasing samarium.

The high (BH)<sub>max</sub> values for the samples E, F, and G reflect the higher density of those samples (Fig. 1 or Table II). The coercive force generally follows the density trend, the exception being Sample H (17.08 at. % Sm) where the coercive force dropped and the density remained at a high level. At substantially higher sintering temperatures, a high H<sub>c1</sub> will not occur, even though higher densities will be achieved.

#### Lattice Parameters vs Temperature

The change of lattice parameters over the temperature range 77° to 300°K are plotted in Fig. 3. The a<sub>0</sub> and c<sub>0</sub> parameters increase with increasing temperature but the c/a ratio decreases with increasing temperature. The thermal expansion coefficients calculated from these data for the temperature range -20° to +24°C are:

$$\alpha_{a_0} = 12.24 \times 10^{-6} / ^\circ\text{C}$$

$$\alpha_{c_0} = 4.00 \times 10^{-6} / ^\circ\text{C}$$

$$\alpha_{\text{vol.}} = 28.94 \times 10^{-6} / ^\circ\text{C}$$

#### SUMMARY

We conclude that the peak coercive force and energy product values occur when the alloy composition is close to the Co<sub>6</sub>Sm-Co<sub>7</sub>Sm<sub>2</sub> boundary (16.8 at. % Sm after adjustment for the formation of Sm<sub>2</sub>O<sub>3</sub>).

The highest magnetic properties have been achieved for samples with a small amount of Co<sub>7</sub>Sm<sub>2</sub>. Samples located in the single phase, Co<sub>6</sub>Sm region or with more than a few volume percent of Co<sub>7</sub>Sm<sub>2</sub> have lower density when sintered under similar conditions and lower magnetic properties. Previously we observed a similar correlation and postulated that the high coercive force and rapid sintering observed in the hyperstoichiometric alloys may be due to the presence of cobalt-vacancy-clusters in the grain-boundary region.<sup>(4)</sup>

The change of the x-ray lattice parameters over the range 77° to 300°K was measured, and thermal expansion coefficients were calculated. The a-axis thermal expansion being about three times that of the c-axis.

#### ACKNOWLEDGMENTS

This study was sponsored by the Advanced Projects Agency of the Department of Defense and was monitored by the Air Force Materials Laboratory, MAYE, under Contract F33615-70-C-1626.



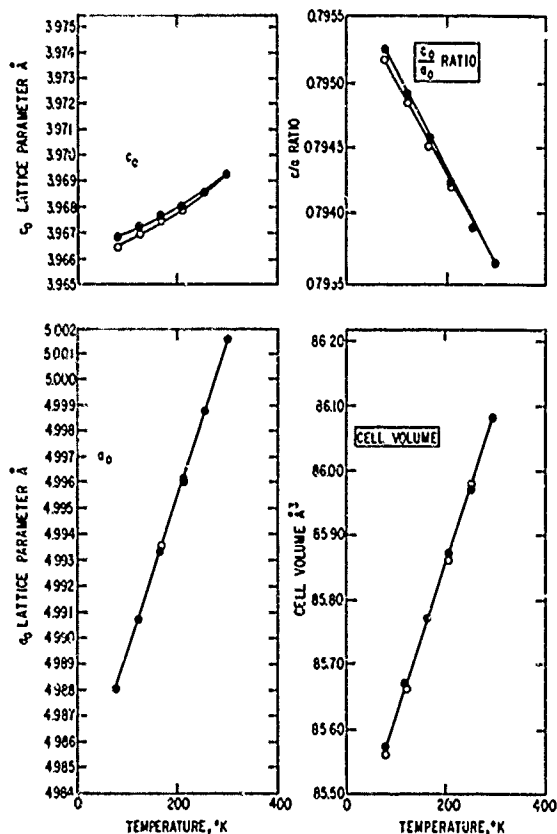


Fig. 3 Change of x-ray parameters with temperature for two Co-Sm samples. The o points are for a 16.8 at. % Sm sample, and the ● points are for a 16.7 at. % Sm sample.

The authors wish to thank J. T. Geertsen, R. T. Laing, R. P. Laforce, and W. F. Moore for the preparation of alloys, test samples, heat treatment, and magnetic testing.

We acknowledge the valuable contributions of the following: S. F. Bartram and R. Goehner for x-ray data; W. E. Balz, B. H. Kindl, and D. H. Wilkins for chemical analyses; J. G. Smeggil and A. Ritzer for metallographic data; and J. J. Becker, J. G. Smeggil, and J. D. Livingston for helpful technical discussions.

#### REFERENCES

1. M. G. Benz and D. L. Martin, *Appl. Phys. Letters* **17**, 176 (1970).
2. R. E. Cech, *J. Appl. Phys.* **41**, 5247 (1970).
3. J. K. Das, *IEEE Trans. Magnetics* **MAG-7** 482 (1971).
4. M. G. Benz and D. L. Martin, *J. Appl. Phys.* **43**, 3165 (1971).
5. K. H. J. Buschow and A. S. Van Der Goot, *J. Less-Common Metals* **14**, 323 (1968).
6. M. U. Cohen, *Rev. Sci. Instr.* **8**, 68 (1935); *Rev. Sci. Instr.* **7**, 155 (1936); *Z. Krist. (A)*, **94**, 288 (1936).
7. E. R. Jette and F. Foote, *J. Chem. Phys.* **3**, 605 (1935).
8. H. Umbayashi and V. Fujimura, *Jap. J. Appl. Phys.* **10**, 1585 (1971).
9. A. E. Austin and J. F. Miller, *Tech. Rept. AFML-TR-72-132*, July 1972, Air Force Materials Lab., Wright-Patterson Air Force Base, Ohio.
10. W. A. J. J. Velge and K. H. J. Buschow, *J. Appl. Phys.* **39**, 1717 (1968).
11. S. E. Haszko, *Trans. AIME* **218**, 763 (Aug. 1960).